holic and water hydrogen atoms were not included in the final refinement. The final values of the positional parameters for M = Sm are given in Table VII.

$[EuCl_3(EO4)]$. The space group was determined to be either the centric $P\bar{1}$ or acentric $P1$. Subsequent solution and successful refinement of the structure was carried out in the centric space group $P\bar{1}$. Least-squares refinement with isotropic thermal parameters led to $R = 0.062$. The ethylene group containing C(7) and C(8) was found to be disordered. Two orientations were resolved for this group and refined with 50% occupancy in alternate least-squares cycles of refinement. The alcoholic hydrogen atoms were not included in the final refinement. The final values of the positional parameters are given in Table VIII.

$[Tm(OH_2)_{4-x}(OHMe)_x(EO4)]Cl_3\cdot(1-x)(H_2O)$ ($x = 0.60$). The space group was determined to be the centric $P2_1/c$ from the systematic absences. An interesting disorder was observed during the initial stages of refinement involving O(9) and the uncoordinated O(10). It was determined that O(9) was a water molecule in some of the Tm coordination spheres and a methanol group in others. Refinement of the occupancy factors resulted in 60% occupancy for the methanol group and 40% occupancy for the water molecule. The different hydrogen-bonding capabilities of these molecules resulted in further disorder in the unit cell. O(10), an uncoordinated water molecule has 40% occupancy, corresponding to the occupancy of O(9) as a water molecule to which it is hydrogen bonded. The methyl hydrogen atoms were included as a rigid group with rotational freedom at the bonded carbon atom (C-H = 0.95 Å, $B = 5.5$ Å^2). The disordered methyl C(9) and O(9) water molecule hydrogen atoms were not included in the final refinement. The final values of the positional parameters are given in Table IX.

$[LuCl_2(EO4)]Cl\cdot H_2O$. The space group was determined to be the centric $P2_1/c$ from the systematic absences. Least-squares refinement with isotropic thermal parameters led to $R = 0.049$. The final values of the positional parameters are given in Table X.

Acknowledgment. We are grateful to the donors of the Petroleum Research Fund, administered by the American Chemical Society, for support of this work and to the American Chemical Society's Project SEED for financial assistance to E.R. The U.S. National Science Foundation's Chemical Instrumentation Program provided funds used to purchase the diffractometer.

Supplementary Material Available: Tables SI-SCXXV, listing bond distances and angles, hydrogen-bonding contact geometries, fractional coordinates not listed in the text, hydrogen atom coordinates, thermal parameters, and least-squares planes results (173 pages); tables of observed and calculated structure factors or amplitudes (197 pages). Ordering information is given on any current masthead page.

Contribution from the Department of Chemistry, Michigan State University, East Lansing, Michigan 48824

Synthesis, X-ray Structure Determination, and Spectroscopy of the Silver(I) Polyselenides $[(Ph_4P)Ag(Se_4)]_n$, $[(Me_4N)Ag(Se_5)]_n$, $[(Et_4N)Ag(Se_4)]_4$, and $(Pr_4N)_2[Ag_4(Se_4)_3]$. Extreme Structure Dependence on Counterion Size

Song-Ping Huang and Mercouri G. Kanatzidis*

Received June 25, 1990

The reaction of sodium pentaselenide with silver nitrate in dimethylformamide (DMF) was investigated. The addition of various counterions, Ph_4P^+, Me_4N^+, Et_4N^+, and Pr_4N^+, to this common reaction solution resulted in the isolation of four new soluble silver(I) polyselenide complexes, $[(Ph_4P)Ag(Se_4)]_n$ (I), $[(Me_4N)Ag(Se_5)]_n$ (II), $[(Et_4N)Ag(Se_4)]_4$ (III), and $(Pr_4N)_2[Ag_4(Se_4)_3]$ (IV), in high yield. Compound I (85% in yield) crystallizes in the monoclinic space group $P2_1/c$ with unit cell dimensions $a = 14.145$ (3) Å, $b = 7.076$ (2) Å, $c = 24.939$ (5) Å, $\beta = 105.23$ (2)°, and $V = 2408$ Å^3. Compound II (93% in yield) crystallizes in the monoclinic space group Cc with unit cell dimensions $a = 11.350$ (2) Å, $b = 18.764$ (3) Å, $c = 7.434$ (1) Å, $\beta = 124.59$ (1)°, and $V = 1303$ Å^3. Compounds III and IV (96% and 76% in yield, respectively) belong to the monoclinic space group $P2_1/n$ with unit cell dimensions $a = 16.229$ (3) Å, $b = 11.480$ (5) Å, $c = 17.171$ (3) Å, $\beta = 106.06$ (1)°, and $V = 3074$ Å^3 and $a = 10.493$ (2) Å, $b = 24.573$ (3) Å, $c = 17.499$ (1) Å, $\beta = 93.84$ (1)°, and $V = 4502$ Å^3, respectively. All structures were solved and refined by direct methods and Fourier techniques. All non-hydrogen atoms were refined anisotropically, and all hydrogen atoms were calculated and included but not refined. Refinement by full-matrix least-squares methods on these structures gave final R values of 7.5% for I, 5.2% for II, 2.8% for III, and 3.3% for IV. The four compounds are divided into two different structural categories: one-dimensional chains, $[(Ph_4P)Ag(Se_4)]_n$ and $[(Me_4N)Ag(Se_5)]_n$, and discrete molecular clusters, $[(Et_4N)Ag(Se_4)]_4$ and $(Pr_4N)_2[Ag_4(Se_4)_3]$. The structures of these four silver(I) polyselenide compounds feature two types of coordination spheres for the Ag atoms, trigonal planar and tetrahedral. Compound I consists of infinite macroanionic chains separated by the cation Ph_4P^+, forming a unique one-dimensional structure containing five-membered $AgSe_4$ rings. These rings are generated from each other by a 2-fold screw axis operation. Each $[Ag(Se_4)]_n^{n-}$ chain contains trigonal-planar Ag^+ atoms. Similarly, compound II is a one-dimensional polymer consisting of $AgSe_5$ as repeat units in which $AgSe_4$ forms a five-membered ring. The $[Ag(Se_5)]_n^{n-}$ chain can be generated by a 2-fold screw axis along the chain direction. The Ag^+ atoms in this structure adopt a tetrahedral coordination geometry. Compound III is molecular. The anion $[Ag(Se_4)]_4^{4-}$ possesses a crystallographic inversion center. Four silver atoms are symmetrically disposed around the inversion center, forming a planar rhombus. The structure features two different kinds of Ag coordination, Ag(1) and Ag'(1) are tetrahedrally coordinated, while the other two Ag(2) and Ag'(2) possess a trigonal-planar coordination. The $[Ag_4(Se_4)_3]^{2-}$ anion features a tetrahedral array of Ag atoms "glued" together by three Se_4^{2-} ligands, forming a Ag_4Se_6 central adamantane-like core in which all Ag^+ ions assume a trigonal-planar coordination. We found a correlation of counterion size and Ag coordination number in these compounds. The smaller the counterions, the higher the silver coordination number. Variable-temperature ^{77}Se NMR spectra of I-IV are reported. The IR spectra of the compounds exhibit two absorptions at ~265 and ~195 cm^{-1}. The former is assigned tentatively to the ν_{Se-Se} vibration. I-III have similar UV/vis spectra in DMF with two absorptions at ~450 and ~630 nm, while IV has a featureless spectrum. Thermal gravimetric analysis data are reported.

1. Introduction

Not only is the coordination chemistry of metal polyselenides or polytellurides less well developed when compared to that of polysulfides[1] but, most interestingly, it does not exactly parallel that of metal polysulfides.[2] It is quite common that a given metal polysulfide compound does not possess a corresponding polyselenide or polytelluride analogue. Plausible reasons are (a) the propensity for catenation of chalcogen atoms decreases from S to Te, which greatly affects Q_x^{2-} ligand sizes, (b) the reduction potentials required to split the Q-Q bonds vary with the nature

(1) (a) Müller, A. *Polyhedron* **1986**, *5*, 323-340. (b) Müller, A.; Diemann, E. *Adv. Inorg. Chem. Radiochem.* **1987**, *31*, 89-122. (c) Draganjac, M.; Rauchfuss, T. B. *Angew. Chem., Int. Ed. Engl.* **1985**, *24*, 742-757.

(2) Ansari, M. A.; Ibers, J. A. *Coord. Chem. Rev.* **1989**, *100*, 223-266.

0020-1669/91/1330-1455$02.50/0

of the element and the ligand size, resulting in different internal redox chemistry in various metal/Q_x^{2-} systems, and (c) the increase of the Q–Q bond lengths from S to Te can affect the chemical nature and dimensions of the Q_x^{2-} ligands. The only few existing isostructural examples are found in the $[M(Q_4)_2]^{2-}$ (M = Zn, Cd, Hg; Q = S, Se, Te),[3] $Ni(Q_4)_2^{2-}$[4] (Q = S, Se), $Fe_2Q_{12}^{2-}$[5,6] (Q = S, Se), and Mo/Q_4^{2-} systems[7] (Q = S, Se, Te). In some cases, the structures of metal polyselenides or polytellurides turned out to be more novel. Typical homoleptic metal polyselenide or polytelluride complexes include $[Fe_2Se_{12}]^{2-}$,[5] $[W_2Se_y]^{2-}$ (y = 9, 10),[8] $[V_2Se_{13}]^{2-}$,[9] $[MQ(Se_4)_2]^{2-}$ (M = Mo, W; Q = O, S, Se),[7] $[M(Se_4)_n]^{2-}$ (n = 2, M = Zn, Cd, Hg;[3] n = 3, M = Pt,[10] Sn[11]), $[Cr_3Q_{24}]^{3-}$ (Q = Se, Te),[12] $[Hg_2Te_5]^{2-}$,[13] $[Hg_4Te_{12}]^{4-}$,[13] $[Au_2Te_2]^{2-}$,[14] $[NbTe_{10}]^{3-}$,[15] $[In_2Se_{21}]^{4-}$,[16] and $[Au_2Se_{10}]^{2-}$.[17]

Recently, there has been a renewed interest in the homo- and heteroatomic main-group polyanions (Zintl anions) derived from the Zintl phases.[18] The extraction of the Zintl phases, such as M_2Q_x (M = alkali metal, Q = Se, Te, x = 4–6), generates solutions that contain polyselenide or polytelluride anions suitable for use as ligands. M_2Q_x compounds are obtained from either high-temperature or liquid ammonia reactions of alkali metals and chalcogens. They dissolve in basic solvents such as ethylene diamine (en) and dimethylformamide (DMF).

The fact that reactions involving heavier polychalcogenide ligands and late transition and main-group metals had not been explored to any significant extent prompted us to undertake an investigation into the synthesis of new metal polyselenide and polytelluride complexes of these metals. We chose the coinage metals as our starting point for new soluble metal polyselenide and polytelluride complexes because, prior to our work, there had been no such complexes and because the corresponding polysulfides present one of the most fruitful triads in the periodic table,[19] especially Cu^+ and Ag^+, which have become the everlasting target of new cluster preparation.[20] This paper describes the isolation and characterization of a series polyselenide compounds of silver, i.e. $[(Ph_4P)Ag(Se_4)]_n$, $[(Me_4N)Ag(Se_5)]_n$, $[(Et_4N)Ag(Se_4)]_4$, and $(Pr_4N)_2[Ag_4(Se_4)_3]$. In this system we have identified a correlation of metal coordination geometry with counterion size. This and other work on the synthesis and structural characterization of metal polyselenide complexes have been published in preliminary form.[16,17,21,22]

2. Experimental Section

2.1. Reagents. Chemicals in this work, other than solvents, were used as obtained: (i) selenium, 99.999% purity, American Smelting and Refining Co., Denver, CO; (ii) sodium metal, analytical reagent, Mallinckrodt Inc., Paris, KY; (iii) silver nitrate, reagent ACS, Sargent-Welch Scientific Co., Skokie, IL; (iv) tetraphenylphosphonium chloride (Ph_4PCl), 98% purity, tetramethylammonium chloride (Me_4NCl), 97% purity, tetraethylammonium bromide (Et_4NBr), 98% purity, and tetrapropylammonium bromide (Pr_4NBr), 97% purity, Aldrich Chemical Co., Inc., Milwaukee, WI. DMF (analytical reagent, Mallinckrodt Inc., Paris, KY) was stored over 4-Å Linde molecular sieves for several days and then distilled under reduced pressure at ~30 °C. The first 50 mL of distillate was discarded. Diethyl ether (ACS anhydrous, Columbus Chemical Industries Inc., Columbus, WI) was distilled after being refluxed with potassium metal, benzophenone, and triethylene glycol dimethyl ether for 12 h.

2.2. Synthesis. All syntheses were carried out under a dry nitrogen atmosphere in a Vacuum Atmospheres Dri-Lab glovebox. Elemental analyses were performed by Galbraith Analytical Laboratories, Knoxville, TN. At the beginning of this work, the starting materials M_2Se_x (M = Na, K; x = 4–6) were prepared by reacting the stoichiometric amounts of selenium with alkali metals in sealed Pyrex tubes at 450 °C. The DMF-extracted solutions of such polyanions were used for reactions with transition-metal ions. However, the exothermic reactions at such temperatures often cause cracks in the tubes and the alloy products usually leave some insoluble residue, which makes the stoichiometric control of reactions difficult. Subsequently, we used a liquid-ammonia method.

Sodium Pentaselenide, Na_2Se_5. An 18-g (~0.23-mol) sample of elemental selenium was combined with 2.2 g (~0.10 mol) of sliced sodium metal under nitrogen in a round-bottom flask equipped with a Teflon valve and a stirbar. A 80-mL volume of liquid ammonia was condensed into the flask at −78 °C (dry ice/acetone bath), and the mixture was stirred for a couple of hours or until the alkali metal had dissolved. When a dark green solution formed, the NH_3 was removed by evaporation at room temperature (by allowing the cold bath to warm slowly) under a flow of nitrogen. The resulting solid was dried in vacuo, flame-dried, and ground to a fine powder in the glovebox. The black microcrystalline powder dissolves in DMF and CH_3CN.

Tetraphenylphosphonium (Tetraselenido)argentate(I), $[(Ph_4P)Ag(Se_4)]_n$ (I). An amount of Na_2Se_5 (0.27 g, 0.61 mmol) was dissolved in a 50-mL DMF solution of Ph_4PCl (0.22 g, 0.60 mmol). To this solution was added dropwise a 10-mL DMF solution of $AgNO_3$ (0.05 g, 0.30 mmol). The resulting red-brown solution was shaken for ca. 10 min. Following filtration, 80 mL of ether was layered over the solution to induce crystallization. When the mixture was left to stand at room temperature for 3 days, red needles (up to 2 mm in length) formed. They were isolated by filtration and washed with ether (0.195 g, 85% yield). No recrystallization was deemed necessary. Anal. Calcd for $C_{24}H_{20}PAgSe_4$: C, 37.76; H, 2.62; Ag, 14.14; Se, 41.41. Found: C,

(3) (a) Adel, J.; Weller, F.; Dehnicke, K. *Z. Naturforsch.* **1988**, *43B*, 1094–1100. (b) Kanatzidis, M. G. *Abstracts of Papers*, 196th National Meeting of the American Chemical Society, Los Angeles, CA, 1988; INORG 469.

(4) Banda, R. M. H.; Cusick, J.; Scudder, M. L.; Craig, D. C.; Dance, I. G. *Polyhedron* **1989**, *8*, 1995–1998.

(5) Strasdeit, H.; Krebs, B.; Henkel, G. *Inorg. Chim. Acta* **1984**, *89*, L11–L13.

(6) Coucouvanis, D.; Swenson, D.; Stremple, P.; Baenziger, N. C. *J. Am. Chem. Soc.* **1979**, *101*, 3392–3394.

(7) (a) Wardle, R. W. M.; Mahler, C. H.; Chau, C.-N.; Ibers, J. A. *Inorg. Chem.* **1988**, *27*, 2790–2795. (b) O'Neal, S. C.; Kolis, J. W. *J. Am. Chem. Soc.* **1988**, *110*, 1971–1973. (c) Hadjikyriacou, A. I.; Coucouvanis, D. *Inorg. Chem.* **1987**, *26*, 2400–2408.

(8) Wardle, R. W. M.; Chau, C.-N.; Ibers, J. A. *J. Am. Chem. Soc.* **1987**, *109*, 1859–1866.

(9) Chau, C.-N.; Wardle, R. W. M.; Ibers, J. A. *Inorg. Chem.* **1987**, *26*, 2740–2741.

(10) Ansari, M. A.; Ibers, J. A. *Inorg. Chem.* **1989**, *28*, 4068–4069.

(11) (a) Banda, R. M. H.; Cusick, J.; Scudder, M. L.; Craig, D. C.; Dance, I. G. *Polyhedron* **1989**, *8*, 1999–2001. (b) Huang, S.-P.; Dhingra, S.; Kanatzidis, M. G. *Polyhedron* **1990**, *9*, 1389–1395.

(12) (a) Flomer, W. A.; O'Neal, S. C.; Pennington, W. T.; Jeter, D.; Cordes, A. W.; Kolis, J. W. *Angew. Chem., Int. Ed. Engl.* **1988**, *27*, 1702–1703. (b) O'Neal, S. C.; Kolis, J. W. *J. Am. Chem. Soc.* **1988**, *110*, 1971–1973.

(13) Haushalter, R. C. *Angew. Chem., Int. Ed. Engl.* **1985**, *24*, 433–435.

(14) Haushalter, R. C. *Inorg. Chim. Acta* **1985**, *102*, L37–L38.

(15) Flomer, W. A.; Kolis, J. W. *J. Am. Chem. Soc.* **1988**, *110*, 3682–3683.

(16) Kanatzidis, M. G.; Dhingra, S. *Inorg. Chem.* **1989**, *28*, 2024–2026.

(17) Kanatzidis, M. G.; Huang, S.-P. *Inorg. Chem.* **1989**, *28*, 4667–4669.

(18) (a) Shäfer, H.; Eisenmann, B.; Müller, W. *Angew. Chem., Int. Ed. Engl.* **1973**, *9*, 694–712. (b) Haushalter, R. C. *J. Chem. Soc., Chem. Commun.* **1987**, 196–197. (c) Haushalter, R. C. *Angew. Chem., Int. Ed. Engl.* **1985**, *24*, 432–433.

(19) (a) Müller, A.; Schladerbeck, N. H.; Krickemeyer, E.; Bögge, H.; Schmitz, K.; Bill, E.; Trautwein, A. X. *Z. Anorg. Allg. Chem.* **1989**, *570*, 7–36. (b) Müller, A.; Baumann, F. W.; Bögge, H.; Schmitz, K. *Z. Anorg. Allg. Chem.* **1985**, *521*, 89–96. (c) Müller, A.; Römer, M.; Bögge, H.; Krickemeyer, E.; Bergmann, D. *J. Chem. Soc., Chem. Commun.* **1984**, 348–349. (d) Müller, A.; Römer, M.; Bögge, H.; Krickemeyer, E.; Schmitz, K. *Inorg. Chim. Acta* **1984**, *B5*, L39–L41.

(20) (a) Block, E.; Gernon, M.; Kang, H.; Liu, S.; Zubieta, J. *J. Chem. Soc., Chem. Commun.* **1988**, 1031–1033. (b) Chada, R. K.; Kumar, R.; Tuck, D. G. *Polyhedron* **1988**, *7*, 1121–1128. (c) Khan, M. A.; Kumar, R.; Tuck, D. G. *Polyhedron* **1988**, *7*, 49–55. (d) Henkel, G.; Krebs, B.; Betz, P.; Fietz, Saatkamp, K. *Angew. Chem., Int. Ed. Engl.* **1988**, *27*, 1326–1329. (e) Gonzalez-Duarte, P.; Sola, J.; Vives, J.; Solans, X. *J. Chem. Soc., Chem. Commun.* **1987**, 1641–1642. (f) Henkel, G.; Betz, P.; Krebs, B. *Angew. Chem., Int. Ed. Engl.* **1987**, *26*, 145–146. (g) Yang, Q.; Tang, K.; Liao, H.; Han, Y.; Chen, Z.; Tang, Y. *J. Chem. Soc., Chem. Commun.* **1987**, 1076–1077. (h) Chada, R. K.; Kumar, R.; Tuck, D. G. *J. Chem. Soc., Chem. Commun.* **1986**, 188–189. (i) Betz, P.; Krebs, B.; Henkel, G. *Angew. Chem., Int. Ed. Engl.* **1984**, *23*, 311–312. (j) Dance, I. G.; Bowmaker, G. A.; Clark, G. R.; Seadon, J. K. *Polyhedron* **1983**, *2*, 1031–1043. (k) Dance, I. G. *Inorg. Chem.* **1981**, *20*, 1487–1492. (l) Coucouvanis, D.; Murphy, C. N.; Kanodia, S. K. *Inorg. Chem.* **1980**, *19*, 2993–2998. (m) Ramli, E.; Rauchfuss, T. B.; Stern, C. L. *J. Am. Chem. Soc.* **1990**, *112*, 4043–4044.

(21) Kanatzidis, M. G.; Huang, S.-P. *J. Am. Chem. Soc.* **1989**, *111*, 760–761.

(22) Kanatzidis, M. G.; Huang, S.-P. *Angew. Chem., Int. Ed. Engl.* **1989**, *28*, 1513–1514.

Table I. Calculated and Observed X-ray Powder Diffraction Patterns for $[(Ph_4P)Ag(Se_4)]_n$

kkl	d_{calcd}, Å	d_{obsd}, Å	I/I_{max}(obsd)
100	13.65	13.50	91
002	12.03	11.93	99
$\bar{1}02$	10.50	10.43	91
102	8.04	8.01	14
200	6.82	6.80	38
$\bar{2}02$	6.74		
$\bar{1}04$	6.13	6.10	100
111	5.91	5.89	30
$\bar{1}13$	5.26	5.24	47
$\bar{1}14$	4.634	4.603	18
014	4.583		
015	3.940	3.928	34
$\bar{2}06$	3.928		
$\bar{2}15$	3.817	3.799	16
$\bar{1}16$	3.583	3.573	21
$\bar{2}16$	3.442	3.434	9
313	3.191	3.181	13
$\bar{4}11$	3.144	3.143	19
$\bar{2}17$	3.106	3.104	24
$\bar{1}24$	3.064	3.002	18
222	2.953		
314	2.947	2.945	18
$\bar{3}17$	2.895	2.818	12
500	2.730	2.721	20

36.89; H, 2.60; Ag, 14.00; Se, 39.36.

Tetramethylammonium (Pentaselenido)argentate(I), $[(Me_4N)Ag(Se_5)]_n$ (II). An amount of Na_2Se_5 (0.27 g, 0.61 mmol) was dissolved in a 50-mL DMF suspension of ground Me_4NCl (0.07 g, 0.60 mmol). After the solution was stirred for 4 h, a 10-mL DMF solution of $AgNO_3$ (0.05 g, 0.30 mmol) was added dropwise. The resulting greenish brown solution was stirred for an additional 4 h and then filtered. To the filtrate was added 100 mL of ether to induce crystallization. When the mixture was left to stand at room temperature for 5 days, dark red needles of $[(Me_4N)Ag(Se_5)]_n$ formed. They were isolated by filtration and washed with ether (0.160 g, 93% yield).

Tetraethylammonium (Tetraselenido)argentate(I), $[(Et_4N)Ag(Se_4)]_4$ (III). An amount of Na_2Se_5 (0.27 g, 0.61 mmol) was dissolved in a 50-mL DMF solution of Et_4NBr (0.13 g, 0.60 mmol). To this solution was added dropwise a 10-mL DMF solution of $AgNO_3$ (0.05 g, 0.30 mmol). The resulting greenish brown solution was stirred for 10 min. After filtration, 80 mL of ether was added. When the mixture was left to stand at room temperature for 2 days, dark red platelets of $[(Et_4N)Ag(Se_4)]_4$ formed. They were isolated as above (0.160 g, 96% yield).

Bis(tetrapropylammonium) Tris(tetraselenido)tetraargentate(I), $(Pr_4N)_2[Ag_4(Se_4)_3]$ (IV). An amount of Na_2Se_5 (0.27 g, 0.61 mmol) was dissolved in a 50-mL DMF solution of Pr_4NBr (0.16 g, 0.60 mmol). To this solution was added dropwise a 10-mL DMF solution of $AgNO_3$ (0.05 g, 0.30 mmol). After being stirred for 10 min, the resulting solution was filtered. To the filtrate was added 80 mL of ether to induce crystallization. When the mixture was left to stand at room temperature for 2 days, red needles of $(Pr_4N)_2[Ag_4(Se_4)_3]$ formed. They were isolated as above (0.200 g, 76% yield).

The homogeneity of all compounds was confirmed by X-ray powder diffraction studies (vide infra).

2.3. Physical Measurements. FT-IR spectra of the complexes were determined as solids in a CsI matrix. Each sample was ground with dry CsI into a fine powder, and a pressure of about 6 tons was applied to the mixture to make a translucent pellet. The spectra were recorded in the far-IR region (600–100 cm^{-1}) with the use of a Nicolet 740 FT-IR spectrometer. UV/vis spectra of the compounds were measured on a Hitachi U-2000 spectrophotometer. The DMF solutions of the complexes were used to determine the extinction coefficients (the samples are insoluble in CH_2Cl_2 and slowly decompose in CH_3CN). Thermal gravimetric analyses (TGA) of the compounds were performed on a Cahn TG System 121. The solid samples were heated to 1000 °C from room temperature at a rate of 5 °C/min under flowing nitrogen.

2.3.1. NMR Spectroscopy. ^{77}Se ($I = {}^1/_2$, natural abundance 7.58%) NMR spectra were obtained on a Varian VXR-500 (superconducting cryomagnet; 11.74 T) pulse spectrometer equipped with a Sun/360 workstation. The spectra were recorded at various temperatures (from −55 °C to 25 °C) by using a broad-band 5-mm probe (frequency range 50–202 MHz). The observing frequency for ^{77}Se was 95.358 MHz. The aquisition time was 0.322 s with a spectral width of 38.35 KHz for ^{77}Se, which gave data point resolution of 1.14 Hz. The pulse width used in these experiments was 6 μs, and no relaxation delay was applied. The number of free induction decays accumulated were 72 000. A line broadening of 80 Hz was applied. The spectra were referenced relative to Me_2Se at $\delta = 0$ ppm in DMF. Solutions of Ph_2Se_2 ($\delta = 460$ ppm) in DMF were used as an external reference. The convention used for the chemical shifts is that a positive sign signifies a shift to high frequency compared to that of the reference compound.

Table II. Calculated and Observed X-ray Powder Diffraction Patterns for $[(Me_4N)Ag(Se_5)]_n$

hkl	d_{calcd}, Å	d_{obsd}, Å	I/I_{max}(obsd)
020	9.38	9.53	18
110	8.36	8.48	100
021	5.13	5.25	8
$\bar{2}21$	4.758	4.792	15
111	4.054	4.083	6
041	3.723	3.747	20
131	3.459	3.476	17
240	3.310	3.325	18
$\bar{3}12$	3.269	3.279	5
$\bar{1}32$	3.099		
310	3.073	3.081	12
$\bar{3}32$	2.932	2.942	10
242	2.903	2.910	8
151	2.784	2.793	12
260	2.599	2.605	8
350	2.397	2.401	9
132	2.334	2.337	5
$\bar{1}72$	2.143	2.145	6
082	1.862	1.861	6

Table III. Calculated and Observed X-ray Diffraction Powder Patterns for $[(Et_4N)Ag(Se_4)]_4$

hkl	d_{calcd}, Å	d_{obsd}, Å	I/I_{max}(obsd)
011	9.42	9.59	100
$\bar{1}11$	8.70	8.87	9
002	8.25	8.39	60
111	7.55	7.69	6
$\bar{2}02$	6.66	6.78	9
$\bar{2}12$	5.76	5.83	43
300	5.20	5.32	19
$\bar{3}02$	5.077	5.014	25
310	4.736	4.788	18
$\bar{3}13$	4.142	4.195	6
$\bar{1}14$	4.021	4.072	18
$\bar{2}14$	3.904	3.930	24
$\bar{3}22$	3.802	3.822	26
312	3.722	3.767	14
$\bar{2}31$	3.448	3.459	24
223	3.284	3.300	35
015	3.172	3.184	28
$\bar{5}11$	3.111	3.111	22
421	3.037	3.026	43
140	2.823	2.831	23
$\bar{6}02$	2.703	2.713	16
240	2.693	2.631	14
$\bar{6}04$	2.539	2.549	25
225	2.500	2.509	17
$\bar{6}15$	2.338	2.336	6
306	2.193	2.205	9
425	2.081	2.083	21
604	1.967	1.965	6
254	1.883	1.888	11
615	1.791	1.793	8

2.4. Crystallographic Studies. All compounds were examined by X-ray powder diffraction for the purpose of phase characterization and identification. A Debye–Scherrer camera was employed to record routine X-ray powder diffraction patterns. Ni-filtered Cu radiation was used. The crystals were ground to fine powder and packed into 0.5-mm glass capillaries, which were sealed and mounted to the standard Debye–Scherrer powder camera (with diameter of 11.46 cm). A Phillips Norelco XRG-5000 X-ray generator operating at 40 kV and 20 mA was used. Approximately, a 6-h exposure time was used. Accurate *d* spacings (Å) for each compound were obtained from the powder patterns recorded on a Phillips XRG-3000 computer-controlled powder diffractometer. To verify the homogeneity of the products, the *d* spacings observed for the bulk materials were compared, and found to be in accord, with the calculated *d* spacings from the single-crystal X-ray structure analysis data.[23] The results are summarized in Tables I–IV. Crystals suitable

Table IV. Calculated and Observed X-ray Powder Diffraction Patterns for $(Pr_4N)_2[Ag_4(Se_4)_3]$

hkl	d_{calcd}, Å	d_{obsd}, Å	I/I_{max}(obsd)
100	10.47	10.33	100
110	9.63	9.50	25
002	8.73	8.97	63
012	8.23	8.16	12
031, $\bar{1}21$	7.42, 7.39	7.59	13
112	6.28	6.17	13
131	5.97	5.90	13
220, 033	4.815, 4.744	4.883	9
104	3.936	3.922	7
054	3.264	3.311	22
$\bar{1}63$	3.226	3.198	13
073	3.006	3.036	35
$\bar{3}33$	2.887	2.839	13
$\bar{2}06$	2.619	2.662	15
$\bar{3}71$	2.467	2.338	9
$\bar{3}46$	2.164	2.115	8
$\bar{4}70$	2.097	2.081	7
267	2.014	2.003	7

for X-ray single-crystal structure analysis were grown by the slow diffusion of diethyl ether into a DMF solution of the filtered reaction mixture. Although the crystals are air-sensitive, they are sufficiently stable to handle in air for a limited amount of time (30 min). Crystals of I–IV were lodged into glass capillaries, which were subsequently flame-sealed. The data for the $[(Me_4N)Ag(Se_5)]_n$, $(Pr_4N)_2[Ag_4(Se_4)_3]$, and $[(Et_4N)Ag(Se_4)]_4$ were collected at Crystalytics, Lincoln, NE, by Dr. C. S. Day using a ω–2θ scan technique. Accurate unit cell parameters for all compounds were obtained from the least-squares refinement on the 2θ, ω, χ, and ϕ values of several (20–25) machine-centered reflections. Intensity data for the crystal of $[(Ph_4P)Ag(Se_4)]_n$ were collected with a Nicolet P3 four-circle automated diffractometer equipped with a graphite-crystal monochromator. The data were collected with the θ–2θ step scan technique.[24] The stability of the experimental setup and crystal integrity were monitored by measuring three standard reflections periodically (every 100 reflections) during the course of data collection. No crystal decay was detected. The raw data were reduced to net intensities. Empirical absorption corrections (ψ scans) were applied, and equivalent reflections were averaged. The structures were solved, at Michigan State University, by direct methods and refined by full-matrix least-squares techniques using the SHELXS-86 and SDP package of crystallographic programs.[25] All calculations were performed on a VAXstation 2000 computer. No disorder was found either in the Ag/Se anions or organic cations in any of the compounds. In all compounds, the hydrogen atom positions were calculated and were included in the structure factor calculations but were not refined. They were given an arbitrary temperature factor which was 1.2 times that of the carbon they are attached to. The complete data collection parameters and details of the structure solution and refinement for all compounds are given in Table V. The coordinates of all atoms in the anions, average temperature factors, and their estimated standard deviations for all compounds are shown in Tables VI–IX.

3. Results

3.1. Description of Structures. Structure of $[(Ph_4P)Ag(Se_4)]_n$ (I). The anion in this material is polymeric, possessing a unique one-dimensional structure. The noninteracting Ph_4P^+ cation has the normal tetrahedral structure and calls for no further comments. Selected bond distances and angles for I are given in Table X.

Figure 1 shows three views of an individual $[AgSe_4]_n^{n-}$ chain. Each chain can be thought of as a corrugated ribbon with the basic repeat unit $AgSe_4$ five-membered ring containing the chelating Se_4^{2-} ligand. Each $AgSe_4$ ring can be generated from its adjacent one by a 2-fold screw operation parallel to the crystal *b* axis. The

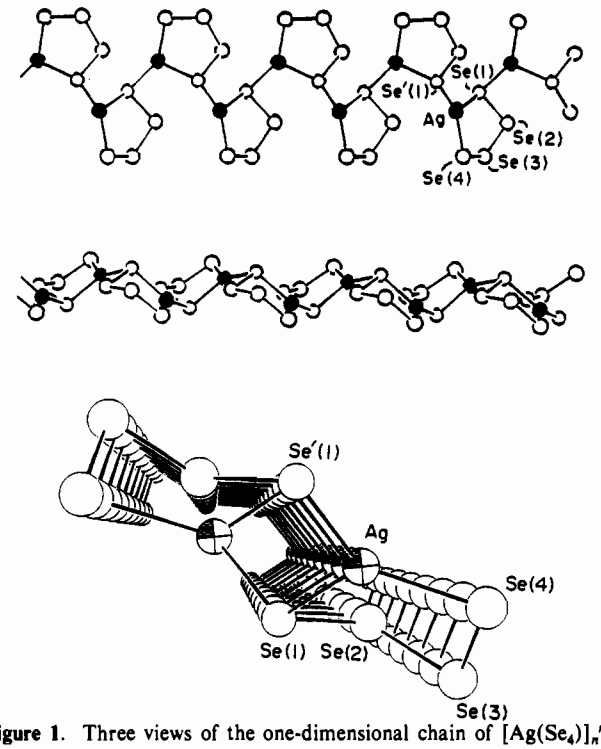

Figure 1. Three views of the one-dimensional chain of $[Ag(Se_4)]_n^{n-}$.

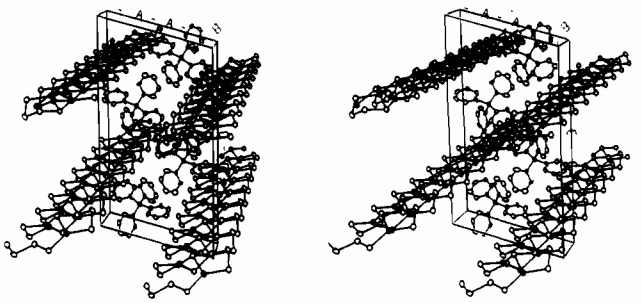

Figure 2. Packing diagram of $[(Ph_4P)Ag(Se_4)]_n$, showing the disposition of the counterions with respect to the chains.

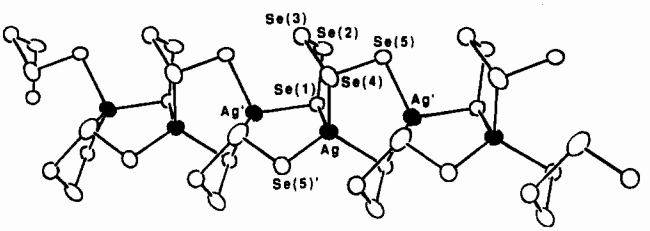

Figure 3. One-dimensional structure with labeling scheme of the $[Ag(Se_5)]_n^{n-}$ chain.

$AgSe_4$ unit polymerizes via a terminal selenium atom in the chelating Se_4^{2-} ligand acting as a bridging ligand for a second Ag atom of a neighboring five-membered $AgSe_4$ unit. This is shown as follows:

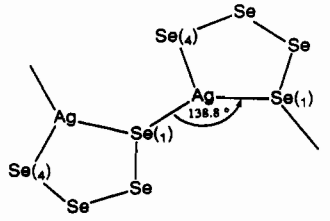

The coordination geometry of the Ag atoms is distorted trigonal planar with two different intra-ring Ag–Se(1) and Ag–Se(4) bonds of 2.672 (2) and 2.553 (2) Å, respectively, and an inter-ring Ag–Se'(1) bond of 2.545 (2) Å. The Se(1)–Ag–Se(4) inter-ring

(23) Smith, D. K.; Nichols, M. C.; Zolensky, M. E. POWD10: A Fortran IV Program for Calculating X-ray Powder Diffration Pattern, version 10. Pennsylvania State University, 1983.
(24) Nicolet XRD Corp. Data Collection Operation Manual, part no. 10062, 1982.
(25) (a) Sheldrick, G. M. In *Crystallographic Computing 3*; Sheldrick, G. M., Kruger, C., Doddard, R., Eds.; Oxford University Press: Oxford, England, 1985; pp 175–189. (b) Frenz, B. A. The Enraf-Nonius CAD4 SDP System. In *Computing in Crystallography*; Delft University Press: Delft, Holland, 1978; pp 64–71.
(26) Banda, R. M. H.; Craig, D. C.; Dance, I. G.; Scudder, M. L. *Polyhedron* **1989**, *8*, 2379–2383.

Table V. Summary of Crystallographic Data for $[(Ph_4P)Ag(Se_4)]_n$,[a] $[(Me_4N)Ag(Se_5)]_n$,[a] $[(Et_4N)Ag(Se_4)]_4$,[a] and $(Pr_4N)_2[Ag_4(Se_4)_3]$[b]

	compd			
	I	II	III	IV
formula	$C_{24}H_{20}PAgSe_4$	$C_4H_{12}NAgSe_5$	$C_{32}H_{80}N_4Ag_4Se_{16}$	$C_{24}H_{56}N_2Ag_4Se_{12}$
fw	762.92	576.71	2215.16	1751.24
a, Å	14.145 (3)	11.350 (2)	16.229 (3)	10.493 (2)
b, Å	7.076 (2)	18.764 (3)	11.480 (5)	24.573 (3)
c, Å	24.939 (5)	7.434 (1)	17.171 (3)	17.499 (1)
α, deg	90.00	90.00	90.00	90.00
β, deg	105.23 (2)	124.59 (1)	106.06 (1)	93.84 (1)
γ, deg	90.00	90.00	90.00	90.00
Z; V, Å	4; 2408	4; 1303	2; 3074	4; 4502
λ	1.5412	0.71073	0.71073	0.71073
space group	$P2_1/c$ (No. 14)	Cc (No. 9)	$P2_1/n$ (No. 14)	$P2_1/n$ (No. 14)
D_{calcd}, g/cm^3	2.104	2.537	2.394	2.585
μ, cm^{-1}	147.0 (Cu Kα)	90.4 (Mo Kα)	106.5 (Mo Kα)	113.3 (Mo Kα)
$2\theta_{max}$, deg	110 (Cu Kα)	44 (Mo Kα)	45 (Mo Kα)	46 (Mo Kα)
final R/R_w, %	7.5/7.6	5.2/5.7[c]	2.8/3.0	3.3/4.0

[a] At 25 °C. [b] At −125 °C. [c] This enantiomorph gave the lowest R.

Table VI. Fractional Atomic Coordinates and B_{eq} Values for the Atoms of the Anion in $[(Ph_4P)Ag(Se_4)]_n$ with Estimated Standard Deviations in Parentheses

atom	x	y	z	B_{eq},[a] Å^2
Ag	0.1029 (1)	0.0322 (3)	0.26700 (6)	4.28 (4)
Se(1)	−0.0071 (2)	0.2544 (3)	0.19703 (9)	3.82 (5)
Se(2)	−0.1370 (2)	0.0360 (4)	0.1860 (1)	4.49 (6)
Se(3)	−0.2714 (2)	0.2100 (4)	0.1352 (1)	5.26 (6)
Se(4)	−0.2848 (2)	0.4705 (5)	0.1917 (1)	5.44 (7)

[a] B values for anisotropically refined atoms are given in the form of the isotropic equivalent displacement parameter defined as $B_{eq} = (4/3)[a^2B(1,1) + b^2B(2,2) + c^2B(3,3) + ab(\cos\gamma)B(1,2) + ac(\cos\beta)B(1,3) + bc(\cos\alpha)B(2,3)]$.

Table VII. Fractional Atomic Coordinates and B_{eq} Values for the Atoms of the Anion in $[(Me_4N)Ag(Se_5)]_n$ with Estimated Standard Deviations in Parentheses

atom	x	y	z	B_{eq},[a] Å^2
Ag	0.648	0.01915 (8)	0.192	3.33 (3)
Se(1)	0.2918 (2)	0.4333 (1)	0.5305 (3)	2.95 (4)
Se(2)	0.6800 (3)	0.8244 (1)	0.3759 (4)	5.11 (5)
Se(3)	0.4367 (3)	0.1505 (2)	0.6387 (4)	6.83 (6)
Se(4)	0.4230 (2)	0.0662 (1)	0.3916 (4)	4.48 (5)
Se(5)	0.4804 (2)	0.8783 (1)	0.6714 (3)	3.21 (4)

[a] B values for anisotropically refined atoms are given in the form of the isotropic equivalent displacement parameter defined as $B_{eq} = (4/3)[a^2B(1,1) + b^2B(2,2) + c^2B(3,3) + ab(\cos\gamma)B(1,2) + ac(\cos\beta)B(1,3) + bc(\cos\alpha)B(2,3)]$.

Table VIII. Fractional Atomic Coordinates and B_{eq} Values for the Atoms of the Anion in $[(Et_4N)Ag(Se_4)]_4$ with Estimated Standard Deviations in Parentheses

atom	x	y	z	B_{eq},[a] Å^2
Ag(1)	0.50990 (5)	0.11510 (8)	0.03740 (5)	4.27 (2)
Ag(2)	0.17671 (5)	0.51551 (7)	0.47829 (5)	3.99 (2)
Se(1)	0.58260 (6)	−0.0973 (1)	0.11973 (6)	3.62 (2)
Se(2)	0.41135 (6)	0.1569 (1)	0.13352 (6)	3.94 (2)
Se(3)	0.52116 (7)	0.1431 (1)	0.81463 (6)	4.73 (3)
Se(4)	0.17432 (7)	0.1121 (1)	0.96349 (7)	4.44 (3)
Se(5)	0.32977 (7)	0.3238 (1)	0.08419 (6)	4.06 (2)
Se(6)	0.31070 (7)	0.7568 (1)	0.43760 (7)	4.89 (3)
Se(7)	0.84383 (6)	0.6964 (1)	0.48010 (7)	4.05 (2)
Se(8)	0.10307 (7)	0.2103 (1)	0.39467 (8)	5.10 (3)

[a] B values for anisotropically refined atoms are given in the form of the isotropic equivalent displacement parameter defined as $B_{eq} = (4/3)[a^2B(1,1) + b^2B(2,2) + c^2B(3,3) + ab(\cos\gamma)B(1,2) + ac(\cos\beta)B(1,3) + bc(\cos\alpha)B(2,3)]$.

angle of 138.8° is unusually large. This, coupled with the significantly lengthened Ag–Se(4) intra-ring bond, represents a slight departure from the ideal trigonal-planar coordination geometry around the Ag atom toward linear geometry. The bonding geometry around the bridging Se(1) atom is trigonal pyramidal. The conformation of the $AgSe_4$ ring is best described as an "envelope" with the Se(2) atom lying 2.21 (4) Å above the least-squares Se(1)/Ag/Se(4)/Se(3) plane. Figure 2 represents the packing of the $[Ag(Se_4)]_n^{n-}$ chains in the unit cell. The infinite anionic chains are well separated by the Ph_4P^+ cations and are spaced ca. 12 Å apart.

Table IX. Fractional Atomic Coordinates and B_{eq} Values for the Atoms of the Anion in $(Pr_4N)_2[Ag_4(Se_4)_3]$ with Estimated Standard Deviations in Parentheses

atom	x	y	z	B_{eq},[a] Å^2
Ag(1)	0.18827 (9)	0.86463 (4)	0.31979 (5)	1.72 (2)
Ag(2)	0.26741 (9)	0.92179 (4)	0.17869 (5)	1.91 (2)
Ag(3)	0.46105 (9)	0.85165 (4)	0.26831 (5)	2.16 (2)
Ag(4)	0.24345 (9)	0.79240 (4)	0.18653 (5)	2.00 (2)
Se(1)	0.4031 (1)	0.45745 (5)	0.23346 (7)	1.83 (2)
Se(2)	0.2960 (1)	0.51191 (5)	0.13746 (7)	2.26 (3)
Se(3)	0.5855 (1)	0.01616 (5)	0.63386 (8)	2.43 (3)
Se(4)	0.5977 (1)	0.10943 (5)	0.60391 (7)	1.93 (2)
Se(5)	0.4964 (1)	0.08100 (5)	0.84770 (7)	2.27 (3)
Se(6)	0.5262 (1)	0.14712 (6)	0.94440 (7)	2.60 (3)
Se(7)	0.4160 (1)	0.22175 (6)	0.89485 (8)	2.92 (3)
Se(8)	0.5299 (1)	0.24570 (5)	0.78762 (8)	2.41 (3)
Se(9)	0.4226 (1)	0.27384 (5)	0.21006 (7)	1.87 (2)
Se(10)	0.6089 (1)	0.29369 (6)	0.28897 (7)	2.13 (3)
Se(11)	0.5602 (1)	0.37357 (6)	0.35095 (7)	2.14 (3)
Se(12)	0.3746 (1)	0.35425 (6)	0.41518 (7)	2.18 (3)

[a] B values for anisotropically refined atoms are given in the form of the isotropic equivalent displacement parameter defined as $B_{eq} = (4/3)[a^2B(1,1) + b^2B(2,2) + c^2B(3,3) + ab(\cos\gamma)B(1,2) + ac(\cos\beta)B(1,3) + bc(\cos\alpha)B(2,3)]$.

Table X. Selected Distances (Å) and Angles (deg) in the $[Ag(Se_4)]_n^{n-}$ Anion with Standard Deviations in Parentheses[a]

Ag–Se(1)	2.672 (2)	Se(1)–Se(2)	2.360 (3)
Ag–Se(4)	2.553 (2)	Se(2)–Se(3)	2.339 (3)
Ag–Se′(1)	2.545 (2)	Se(3)–Se(4)	2.358 (4)
Ag–Se (mean)	2.590 (41)	Se–Se (mean)	2.352 (7)
Ag--Ag	4.518 (3)		
Se(1)–Ag–Se′(1)	114.26 (1)	Ag–Se(1)–Se(2)	89.57 (2)
Se(1)–Ag–Se(4)	138.80 (2)	Ag–Se′(1)–Se(2)	94.19 (2)
Se′(1)–Ag–Se(4)	106.60 (2)	Ag–Se(4)–Se(3)	98.33 (2)
Ag–Se(1)–Ag′	119.71 (1)	Ag–Se–Se(mean)	94 (3)
		Se(1)–Se(2)–Se(3)	102.47 (2)
		Se(2)–Se(3)–Se(4)	105.60 (2)
		Se–Se–Se(mean)	104 (2)

[a] The estimated standard deviations in the mean bond lengths and the mean bond angles are calculated by the equations $\sigma_l = [\sum_n (l_n - l)^2/n(n-1)]^{1/2}$, where l_n is the length (or angle) of the nth bond, l the mean length (or angle), and n the number of bonds.

Structure of $[(Me_4N)Ag(Se_5)]_n$ (II). The anion in this material is shown in Figure 3. This structure has a polysulfide analogue in the recently reported $[(Me_4N)Ag(S_5)]_n$.[24] It is also polymeric,

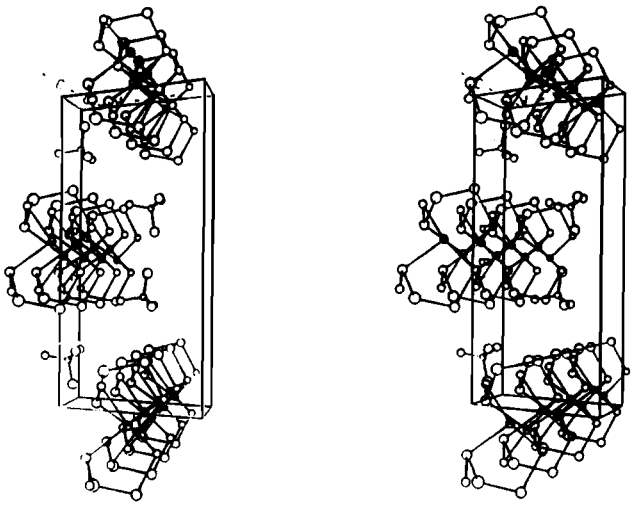

Figure 4. Packing diagram of $[(Me_4N)Ag(Se_5)]_n$, showing the disposition of the counterions with respect to the chains.

Table XI. Selected Distances (Å) and Angles (deg) in the $[Ag(Se_5)]_n^{n-}$ Anion with Standard Deviations in Parentheses[a]

Ag–Se(1)	2.633 (2)	Se(1)–Se(2)	2.334 (3)
Ag–Se(4)	2.756 (2)	Se(2)–Se(3)	2.329 (3)
Ag–Se′(5)	2.648 (27)	Se(3)–Se(4)	2.362 (4)
Ag′–Se(1)	2.670 (3)	Se(4)–Se(5)	2.324 (4)
Ag–Se(mean)	2.677 (3)	Se–Se(mean)	2.337 (12)
Ag–Ag	3.786 (4)		
Se(1)–Ag–Se′(1)	115.40 (7)	Ag–Se(1)–Se(2)	101.30 (8)
Se(1)–Ag–Se(4)	101.86 (8)	Ag–Se(4)–Se(3)	97.90 (10)
Se(1)–Ag–Se′(4)	110.62 (8)	Ag–Se(4)–Se(5)	109.23 (12)
Se′(1)–Ag–Se(4)	122.34 (8)	Ag′–Se(5)–Se(4)	96.50 (10)
Se(1)–Ag–Se′(5)	109.48 (7)	Ag–Se–Se(mean)	100 (3)
Se(4)–Ag–Se′(5)	94.03 (7)	Se(1)–Se(2)–Se(3)	106.02 (14)
Ag–Se(1)–Ag′	91.11 (7)	Se(2)–Se(3)–Se(4)	104.52 (16)
		Se(3)–Se(4)–Se(5)	109.02 (15)
		Se–Se–Se(mean)	107 (1)

[a] See footnote *a* in Table X.

forming an infinite one-dimensional structure with the Me_4N^+ cations situated between the macroanionic chains. The basic repeat unit is $AgSe_5$. The packing of the $[Ag(Se_5)]_n^{n-}$ macroanions in the unit cell is shown in Figure 4, and it is similar to that of $[Ag(Se_4)]_n^{n-}$. The noncentrosymmetric $[Ag(Se_5)]_n^{n-}$ chains run parallel to the crystal *c* axis and are spaced ~6 Å apart by Me_4N^+ cations. Selected bond distances and angles for II are given in Table XI. Despite the six-member atom repeat unit occurring in the chains, the structure contains only five-membered $AgSe_4$ and Ag_2Se_3 rings. The ligation mode of the Se_5^{2-} ligands in the compound differs from that of the Se_4^{2-} ligands present in $[Ag(Se_4)]_n^{n-}$. Each Se_5^{2-} ligand chelates a Ag atom via Se(1) and Se(4) to form a $AgSe_4$ ring. The terminal Se atoms Se(1) and Se(5) serve as bridges to coordinate other Ag atoms. The overall bonding mode of the Se_5^{2-} ligand is shown as follows:

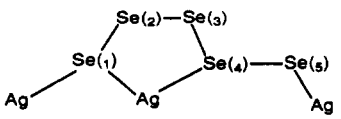

The Se(1) bridges two Ag atoms and assumes a trigonal-pyramidal coordination geometry, while the Se(5) chelates one Ag atom.

The coordination geometry of the Ag atom is tetrahedral with four normal Ag–Se bonds Ag–Se(1) = 2.633 (2) Å, Ag′–Se(1) = 2.670 (3) Å, Ag–Se(4) = 2.756 (2) Å, and Ag–Se′(5) = 2.648 (3) Å. The $AgSe_4$ ring adopts an envelope conformation with the Se(3) atom lying 1.21 Å above the least-squares Se(2)/Se(1)/Ag/Se(4) plane.

Structure of $[(Et_4N)Ag(Se_4)]_4$ (III). In contrast to I and II, the anion in this compound is a discrete tetrameric cluster molecule

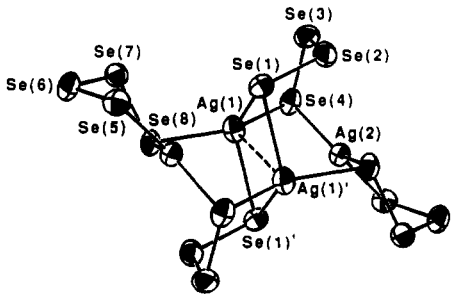

Figure 5. Structure of the $[Ag(Se_4)]_4^{4-}$ cluster with labeling scheme.

Table XII. Selected Distances (Å) and Angles (deg) in the $[Ag(Se_4)]_4^{4-}$ Anion with Standard Deviations in Parentheses[a]

Ag(1)–Se(1)	2.901 (1)	Se(1)–Se(2)	2.331 (2)
Ag(1)–Se′(1)	2.708 (1)	Se(2)–Se(3)	2.341 (2)
Ag(1)–Se(4)	2.644 (1)	Se(3)–Se(4)	2.343 (2)
Ag(1)–Se(8)	2.641 (1)	Se(5)–Se(6)	2.340 (2)
Ag(2)–Se(4)	2.583 (1)	Se(6)–Se(7)	2.336 (2)
Ag(2)–Se′(5)	2.596 (1)	Se(7)–Se(8)	2.350 (2)
Ag(2)–Se′(8)	2.616 (1)	Se–Se(mean)	2.340 (3)
Ag–Se(mean)	2.67 (4)		
Ag(1)–Ag(1)	2.917 (1)		
Ag(1)–Ag(2)	3.178 (1)		
Ag(1)–Ag(2)′	3.482 (1)		
Se(1)–Ag(1)–Se′(1)	117.44 (4)	Ag(1)–Se(1)–Se(2)	100.05 (2)
Se(1)–Ag(1)–Se(4)	95.47 (4)	Ag(1)–Se(4)–Se(3)	98.73 (5)
Se′(1)–Ag(1)–Se(4)	100.43 (4)	Ag(2)–Se(5)–Se(6)	97.19 (5)
Se(1)–Ag(1)–Se(8)	94.76 (4)	Ag(2)–Se(8)–Se(7)	95.87 (4)
Se′(1)–Ag(1)–Se(8)	111.82 (4)	Ag(2)–Se(4)–Se(3)	102.69 (5)
Se(4)–Ag(1)–Se(8)	136.47 (4)	Ag–Se–Se(mean)	99 (1)
Se(4)–Ag(2)–Se′(5)	118.27 (4)	Se(1)–Se(2)–Se(3)	104.31 (6)
Se(4)–Ag(2)–Se′(8)	134.52 (4)	Se(2)–Se(3)–Se(4)	102.42 (6)
Se′(5)–Ag(2)–Se(8)	106.21 (4)	Se(6)–Se(7)–Se(8)	102.53 (6)
Ag(1)–Se(1)–Ag′(1)	62.56 (2)	Se–Se–Se(mean)	103.5 (7)
Ag(1)–Se(4)–Ag(2)	83.55 (2)		
Ag(1)–Se(8)–Ag′(2)	74.40 (2)		

[a] See footnote *a* in Table X.

composed of five-membered $AgSe_4$ rings and featuring two different kinds of Ag coordination. The $[Ag(Se_4)]_4^{4-}$ is situated on a crystallographic inversion center. Figure 5 shows the structure of the anion. A planar rhombus of four Ag atoms, symmetrically disposed around the inversion center, is held together by four Se_4^{2-} ligands. The four Ag atoms in the cluster can be divided into two different pairs according to their coordination environments. One pair containing Ag(1) and Ag′(1) possesses a very distorted tetrahedral coordination. The other group containing Ag(2) and Ag′(2) shows a trigonal-planar coordination. Similarly, the four bridging Se_4^{2-} ligands are not equivalent and split in two sets. In one set, two Se_4^{2-} ligands bridge three silver atoms, Ag(1), Ag′(1), and Ag(2), with atoms Se(1) and Se(4) being of the μ_2 type. In the other set, two Se_4^{2-} ligands are bridging two silver atoms, Ag(1) and Ag(2), each with only one terminal atom, Se(8), being of the μ_2 type. This mode of bridging is similar to that found in I. Selected bond distances and angles for III are given in Table XII.

The tetrahedral geometry around Ag(1) is highly distorted with one very long Ag(1)–Se(1) "bond" at 2.901 (1) Å, a long Ag(1)–Se′(1) bond at 2.708 (1) Å, and two normal bonds Ag(1)–Se(8) and Ag(1)–Se(4) at 2.641 (1) and 2.644 (1) Å, respectively. The Ag(1) atom is displaced considerably from the center of the Se(1)/Se(4)/Se(8)/Se′(1) tetrahedron toward the Se(1)/Se(4)/Se(8) face. Ag(1) lies 1.868 (1) Å above the Se′(1)/Se(4)/Se(8) plane. As a result, the angles around Ag(1) deviate dramatically from the ideal tetrahedral angles. Thus, the geometry around Ag(1) is best described as intermediate between trigonal planar and tetrahedral. The trigonal-planar geometry of the Ag(2) atom can be considered similar to that in $[(Ph_4P)Ag(Se_4)]_n$ with comparable bond lengths and angles (see tables X and XII). The Se_4^{2-} ligands that chelate the Ag(1) atom adopt a twist-boat conformation, while the corresponding ligands chelating the Ag(2)

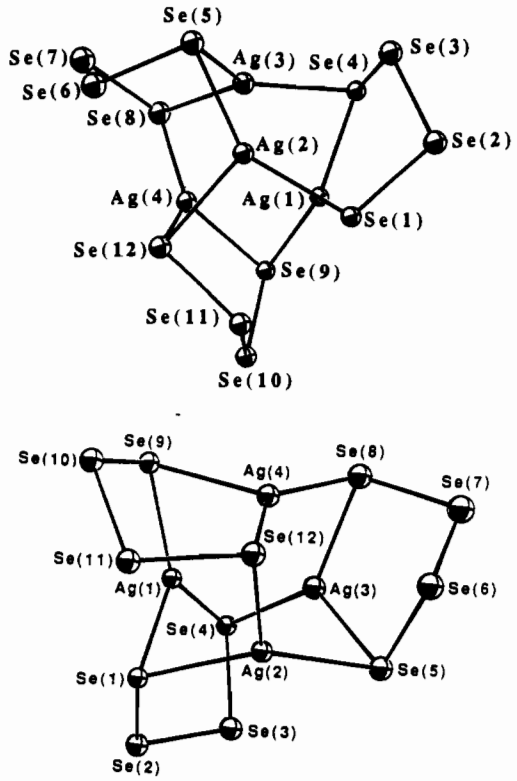

Figure 6. Two views of the structure of the $[Ag_4(Se_4)_3]^{2-}$ cluster with labeling scheme.

Table XIII. Selected Distances (Å) and Angles (deg) in the $[Ag_4(Se_4)_3]^{2-}$ Anion with Standard Deviations in Parentheses[a]

Ag(1)–Se(1)	2.621 (1)	Ag(1)–Ag(2)	3.005 (1)
Ag(1)–Se(4)	2.614 (1)	Ag(1)–Ag(3)	3.074 (1)
Ag(1)–Se(9)	2.554 (1)	Ag(1)–Ag(4)	3.193 (1)
Ag(2)–Se(1)	2.588 (1)	Ag(2)–Ag(3)	3.022 (1)
Ag(2)–Se(5)	2.552 (1)	Ag(2)–Ag(4)	3.017 (1)
Ag(2)–Se(12)	2.710 (1)	Ag(3)–Ag(4)	2.990 (1)
Ag(3)–Se(4)	2.545 (1)		
Ag(3)–Se(5)	2.680 (1)	Se(1)–Se(2)	2.371 (1)
Ag(3)–Se(8)	2.589 (1)	Se(2)–Se(3)	2.311 (1)
Ag(4)–Se(8)	2.567 (1)	Se(3)–Se(4)	2.357 (1)
Ag(4)–Se(9)	2.634 (1)	Se(5)–Se(6)	2.352 (1)
Ag(4)–Se(12)	2.592 (1)	Se(6)–Se(7)	2.306 (1)
Ag–Se(mean)	2.604 (15)	Se(7)–Se(8)	2.366 (1)
		Se(9)–Se(10)	2.367 (1)
		Se(10)–Se(11)	2.316 (1)
		Se(11)–Se(12)	2.361 (1)
		Se–Se(mean)	2.345 (16)

Se(1)–Ag(1)–Se(4)	104.52 (2)	Ag(1)–Se(1)–Ag(2)	70.47 (2)
Se(1)–Ag(1)–Se(9)	122.47 (2)	Ag(1)–Se(4)–Ag(3)	73.14 (2)
Se(4)–Ag(1)–Se(9)	132.97 (2)	Ag(2)–Se(5)–Ag(3)	70.52 (2)
Se(1)–Ag(2)–Se(5)	146.58 (2)	Ag(1)–Se(9)–Ag(4)	71.11 (2)
Se(1)–Ag(2)–Se(12)	101.15 (2)	Ag–Se–Ag(mean)	72.3 (9)
Se(5)–Ag(2)–Se(12)	112.03 (2)		
Se(5)–Ag(3)–Se(4)	119.72 (2)	Se(1)–Se(2)–Se(3)	104.93 (3)
Se(5)–Ag(3)–Se(8)	105.79 (2)	Se(2)–Se(3)–Se(4)	103.32 (3)
Se(4)–Ag(3)–Se(8)	134.14 (2)	Se(5)–Se(6)–Se(7)	103.88 (3)
Se(8)–Ag(4)–Se(9)	117.59 (2)	Se(6)–Se(7)–Se(8)	103.24 (3)
Se(8)–Ag(4)–Se(12)	136.83 (2)	Se(9)–Se(10)–Se(11)	104.38 (3)
Se(9)–Ag(4)–Se(12)	105.40 (2)	Se(10)–Se(11)–Se(12)	105.50 (3)
		Se–Se–Se(mean)	104.3 (4)

[a] See footnote *a* in Table X.

atom remain in the envelope conformation.

Structure of $(Pr_4N)_2[Ag_4(Se_4)_3]$ (IV). Two views of this cluster are shown in Figure 6. Unlike in the related $(Ph_4P)_2[Ag_4(Se_4)_x(Se_5)_{3-x}]$,[27] no disorder or traces of Se_5^{2-} ligands were found in IV. It features a tetrahedral array of silver atoms held together by three Se_4^{2-} ligands, forming a highly distorted Ag_4Se_6 central adamantane-like core in which all Ag atoms assume trigonal-planar coordination. Selected bond distances and angles for IV are given in Table XIII. There is an approximate 3-fold axis of symmetry passing through the Ag(2) and the center of the Ag(1)Se(4)Ag(3)Se(8)Ag(4)Se(9) six-membered ring. In spite of the common coordination geometry, the four silver atoms are linked by three Se_4^{2-} ligands through two different chelating modes. First, each of three Ag atoms, Ag(1), Ag(3), and Ag(4), is chelated by a Se_4^{2-} ligand itself and connected to one another via a terminal selenium atom from each $AgSe_4$ ring (i.e. Se(4), Se(8), and Se(9)). By so doing, a primitive trimeric cluster, $[Ag_3(Se_4)_3]^{3-}$, can be formed shown as follows:

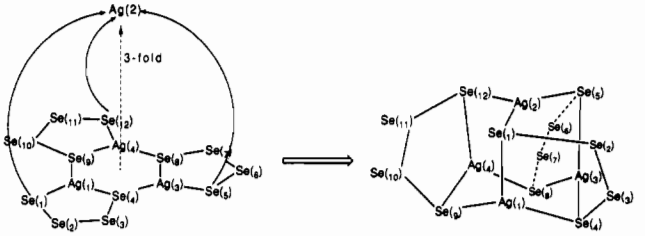

Figure 7. Structural relationship of a $[Ag(Se_4)]_3^{3-}$ trimer and the $[Ag_4(Se_4)_3]^{2-}$ cluster type.

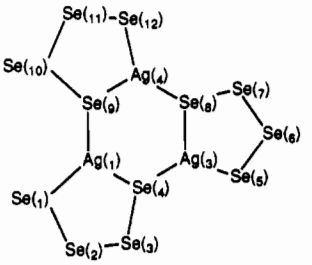

Conceptually, the tetrameric $[Ag_4(Se_4)_3]^{3-}$ can be derived after the fourth Ag atom, Ag(2), is placed on the trimer, approaching along the 3-fold axis, and linked through those unbridged terminal selenium atoms, Se(1), Se(5), and Se(12), by folding up the structure, as shown in Figure 7. Therefore, the Ag(2) atom is chelated by three Se_4^{2-} ligands, while the other Ag atoms are linked by only two of three Se_4^{2-} ligands.

The Ag–Se bond distances in this cluster are similar to those found in $[Ag_4(Se_4)_x(Se_5)_{3-x}]^{2-}$.[27] All angles around the Ag atoms are close to 120° except Se(1)–Ag(2)–Se(5), which is expanded to 147°. Two of the $AgSe_4$ rings in this structure, Ag(1)/Se(1)/Se(2)/Se(3)/Se(4) and Ag(4)/Se(9)/Se(10)/Se(11)/Se(12), are in the envelope conformation with Se(2) and Se(10) lying ~1 Å above the least-squares planes Ag(1)/Se(1)/Se(4)/Se(3) and Ag(4)Se(9)Se(11)Se(12), respectively. The third ring, Ag(3)/Se(5)/Se(6)/Se(7)/Se(8), is found in the half-boat conformation with Se(6) and Se(7) lying 0.55 and 0.79 Å above and below the least-squares plane Se(8)/Ag(3)/Se(5), respectively.

3.2. Synthesis and Spectroscopy. The synthesis of the four Ag^+/polyselenide complexes is readily accomplished by a common reaction between $AgNO_3$ and Na_2Se_5, in the 1:2 ratio in the presence of different quaternary ammonium or quaternary phosphonium cations in DMF according to the following scheme:

$$AgNO_3 + 2Na_2Se_5 + R_4EX \xrightarrow{DMF} [(R_4B)_pAg_x(Se_y)_q]_n + NaCl + NaNO_3 \quad (1)$$

R = Me, Et, Pr, E = N; R = Ph, E = P; X = Cl, Br

Solutions of $[(R_4E)_pAg_x(Se_y)_q]_n$ are red with a green cast (except for IV, which is red) and are air-sensitive. All complexes we characterized by FT-IR, UV/vis, and ^{77}Se NMR spectroscopies.

All the Ag^+/Se_x^{2-} complexes except for $(Pr_4N)_2[Ag_4(Se_4)_3]$ have UV/vis spectra (in DMF) similar to that of Na_2Se_5 or $(Ph_4P)_2Se_5$. The typical UV/vis spectrum in DMF shown in Figure 8 has two absorptions at ~450 (sh) and ~630 nm. (Extinction coefficients for given concentrations are given in Table XIV.) These two absorptions are thought to originate from

(27) Cusick, J.; Scudder, M. L.; Craig, D. C.; Dance, I. G. *Polyhedron* **1989**, *8*, 1139–1141.

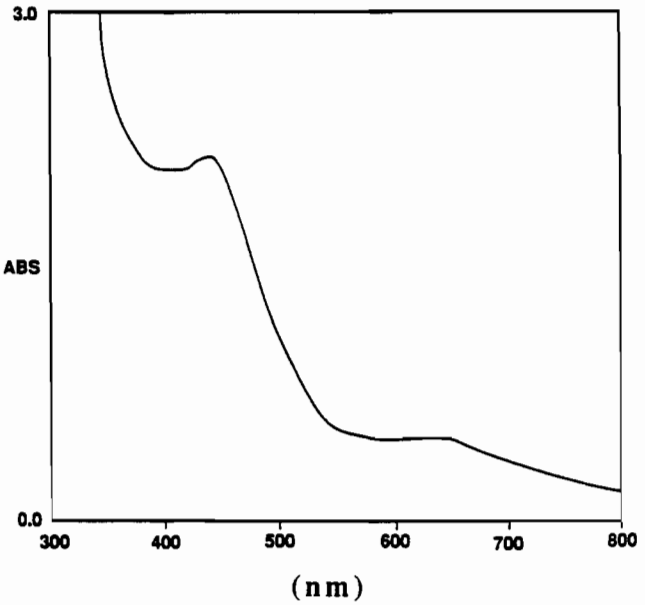

Figure 8. Typical UV/vis spectrum of $[(Et_4N)Ag(Se_4)]_4$ in DMF. I and II have similar spectra.

Table XIV. Summary of Electronic Spectral Data for I–III and $(Ph_4P)_2Se_5$ in DMF Solution at Room Temperature

compd	concn, M	λ_{max}, nm	extn coeff ϵ, $M^{-1}\cdot cm^{-1}$
$[(Me_4N)Ag(Se_5)]_n$	7.801×10^{-3}	450 (sh)	2812
		636	574
$[(Et_4N)Ag(Se_4)]_4$	5.054×10^{-3}	443	4218
		632	937
$[(Ph_4P)Ag(Se_4)]_n$	1.147×10^{-2}	455 (sh)	1749
		640	242
$(Ph_4P)_2Se_5$	1.676×10^{-3}	446	8819
		623	1891

selenium radical anion species $Se_x^{\bullet-}$ present in solution. This is by analogy to the corresponding polysulfide solutions. The UV/vis, Raman, and resonance Raman spectroscopic studies on polysulfides in liquid ammonia or polar solvents such as DMF suggest that different S_x^{2-} ligands are in equilibrium with the radical-anion $S_3^{\bullet-}$ and other species such as S_2^{2-}.[28] A similar equilibrium can be postulated for the dissociation of Se_x^{2-} ligands in DMF.[29] The presence of two UV/vis bands (at room temperature), 450 and 630 nm, in DMF solutions of the three complexes $[(Ph_4P)Ag(Se_4)]_n$, $[(Me_4N)Ag(Se_5)]_n$, and $[(Et_4N)Ag(Se_4)]_4$ indicates that they dissociate in this solvent to form species similar to those existing in S_x^{2-} solutions, as depicted in eq 2. This is not entirely surprising if we consider that monovalent metal ions do not usually form complexes with high stability constants.

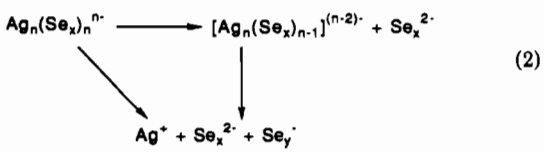

(2)

Contrary to the case for I–III, the UV/vis spectrum of $(Pr_4N)_2[Ag_4(Se_4)_3]$ shows a featureless rising absorbance, indicating that this compound does not dissociate according to eq 2, at least not to the same extend as I–III do. It should be noted that the $[Ag_4(Se_4)_3]^{2-}$ complex has a higher Ag^+/Se_x^{2-} ratio. The excess Ag^+ reduces the total negative charge of the complex and forms a tighter aggregate, which resists extensive dissociation of the Se_4^{2-} ligands. The same applies to $[Cu_4(Se_4)_3]^{2-}$.

All the Ag^+/Se_x^{2-} complexes reported here exhibit an absorption in the far-IR region of the spectrum around 265 cm^{-1} as a common feature. This band can be assigned to a Se–Se stretching vibration by comparison to the spectra of other polyselenide complexes and with that of a free ligand $(Ph_4P)_2Se_5$ (ν_{Se-Se} = 267 cm^{-1}). The ν_{Se-Se} absorbance in this region has been observed previously, by several authors in various compounds, e.g. Se_x^{2-}[30] (x = 1–6) at 285 cm^{-1}, c-Se_6[31] at 253 cm^{-1}, $[Fe_2Se_{12}]^{2-}$[5] at 258 cm^{-1}, and $[Pd(Se_4)_2]^{2-}$[32] at 274 cm^{-1}. In addition, a medium-intensity band around 195 cm^{-1} was found in all the complexes. This might be a possible candidate for an Ag–Se stretching vibration. It should be noted that it is usually difficult to interpret the IR spectra of metal polyselenide complexes without ambiguity. The major difficulties in assigning the observed IR absorbances of metal polyselenides result from the fact that the M–Se and Se–Se stretching frequencies fall in the same low-frequency IR region (200–340 cm^{-1}) and that systematic IR spectroscopic data for the various free ligands (Se_x^{2-}, x = 2–6) and metal selenide complexes are still lacking.

3.3. Thermal Decomposition Studies. All four Ag^+ polyselenides showed well-defined thermal decompositions by thermal gravimetric analysis (TGA). The compounds decompose to form a mixture of Ag_2Se (Ag_2Se-120, naumannite)[33] and elemental Se with release of R_3N and R_2Se. The decomposition commences at different temperatures depending on the counterion. $[(Me_4N)Ag(Se_5)]_n$, $[(Et_4N)Ag(Se_4)]_4$, and $(Pr_4N)_2[Ag_4(Se_4)_3]$ begin to lose weight at ca. 120, 180, and 180 °C, respectively, while $[(Ph_4P)Ag(Se_4)]_n$ is stable up to 300 °C (Figure 11). The dependence of decomposition temperatures upon the nature of the counterions reflects the order of susceptibility of nucleophilic attack of the organic cations by the polychalcogenide ligands. The thermal stability of this series has the following order: $Ph_4P^+ \gg Pr_4N^+ > Et_4N^+ > Me_4N^+$. This is as expected on the basis of considerations of the stability of the alkyl–N and aryl–P bonds in these cations. All final decomposition products (above 400 °C) were found to be, by X-ray powder diffraction, pure Ag_2Se. The final weight loss observed from the TGA diagrams was in excellent agreement with the theoretical value.

4. Discussion

4.1. Availability of Polyselenide Ligands. The initial approach to metal polysulfides usually was to pass a stream of H_2S through an aqueous base (i.e. aqueous NH_3) in the presence of elemental sulfur.[34] The polysulfide solutions generated from such a procedure were then reacted in situ with appropriate metal salts. Although this has been successful in preparing metal polysulfides, it seems to be an expensive, inconvenient, potentially irreproducible, and impractical (H_2Se is extremely poisonous and H_2Te is unstable) route to metal polyselenides or polytellurides. There are several old preparative routes to metal polyselenide compounds: (a) reacting aqueous ammonia solution of excess H_2Se in the presence of Se with an appropriate metal compound, usually metal oxide or metal selenide;[35] (b) using elemental selenium as reagent in an oxidative-addition reaction with a low-valent metal complex;[36] (c) reacting sodium metal (or $LiEt_3BH$[37]) with elemental selenium in DMF in the presence of a metal precursor to form the poly-

(28) (a) Dubois, P.; Lelieur, J. P.; Lepourte, G. *Inorg. Chem.* **1988**, *27*, 73–80. (b) Clark, R. J. H.; Walton, J. R. *J. Chem. Soc., Dalton Trans.* **1987**, 1535–1544. (c) Clark, R. J. H.; Dines, T. J.; Proud, G. P. *J. Chem. Soc., Dalton Trans.* **1983**, 2299–2302.
(29) Kanatzidis, M. G. *Comments Inorg. Chem.* **1990**, *10*, 161–195.
(30) Weller, F.; Adel, J.; Dehnicke, K. *Z. Anorg. Allg. Chem.* **1987**, *548*, 125–132.
(31) Nagata, K.; Tshibashi, K.; Miyamoto, Y. *Jpn. J. Appl. Phys.* **1980**, *19*, 1569–1573.
(32) Kräuter, G.; Dehnicke, K.; Fenske, D. *Chem.-Ztg.* **1990**, *114*, 7–9.
(33) JCPDS International Center for Diffraction Data, Powder Diffraction File 24-1044.
(34) Krause, R. A.; Kozlowski, A. W.; Cronin, J. L. *Inorg. Synth.* **1982**, *21*, 12–16.
(35) Lenher, V.; Fruehan, A. G. *J. Am. Chem. Soc.* **1927**, *49*, 3076–3080.
(36) Ginsberg, A. P.; Linndsell, W. E.; Sprinrle, C. R.; West, K. W.; Cohen, R. L. *Inorg. Chem.* **1982**, *21*, 3666–3681.
(37) (a) Köpf, H.; Block, B.; Schmidt, M. *Chem. Ber.* **1968**, *101*, 272. (b) Shaver, A.; McCall, J. M. *Organometallics* **1984**, *3*, 1823–1829. (c) Bolinger, M. C.; Rauchfuss, T. B. *Inorg. Chem.* **1982**, *21*, 3947–3954.

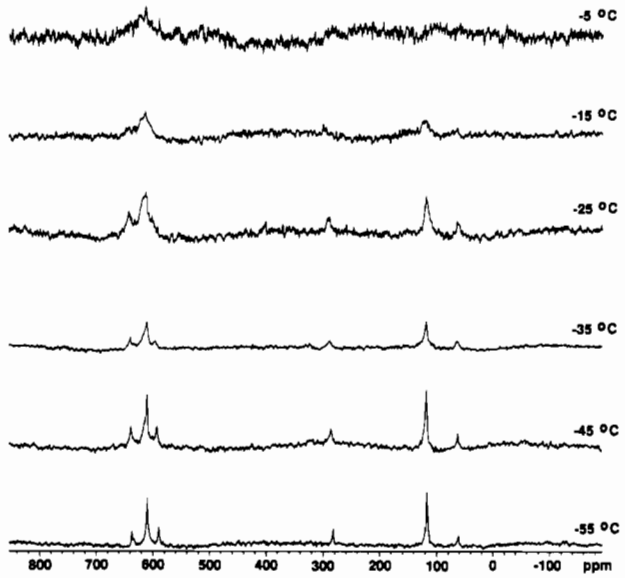

Figure 9. ^{77}Se NMR spectra of $[(Et_4N)Ag(Se_4)]_4$ in DMF as a function of temperature.

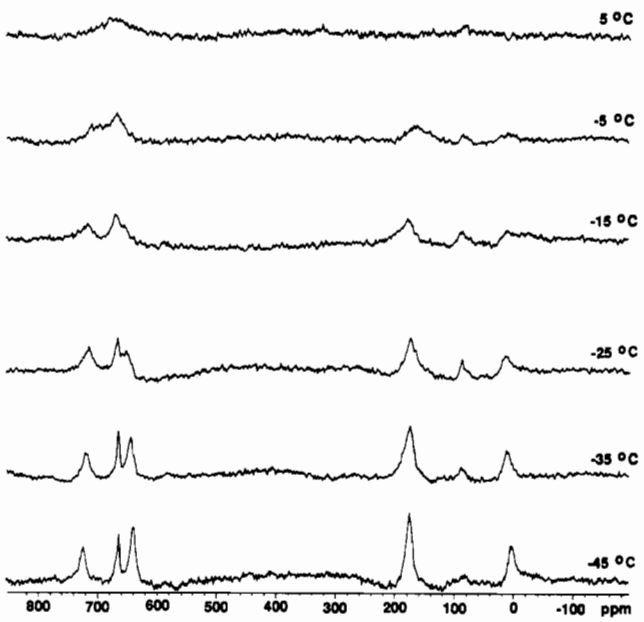

Figure 10. ^{77}Se NMR spectra of $(Pr_4N)_2Ag_4(Se_4)_3$ in DMF as a function of temperature.

selenide complex in situ.[4,5,27,37] Each of them is analogous to (but less convenient than) those of polysulfide complexes. The reaction of Se with Na_2Se to form polyselenide ligands in solution[3a,38] has also been used. Kolis et al.[12] and ourselves used the solvent-extracted Se_x^{2-} polyanions obtained from liquid-ammonia reactions as selenium sources for the introduction of polyselenide ligands to metal ions. In our hands this method provides excellent polychalcogenide anions for synthetic reactions.

4.2. Synthesis of Ag/Se_x Complexes. The successful isolation of four compositionally and structurally different complexes from the common Ag^+/Se_x^{2-} mixture is attributed to the crystallization characteristics of the different organic counterions. These stable counterions supply various cavity sizes in the crystal lattice and force the labile complex anions to adopt appropriate molecular shapes.

Originally, we replaced Et_4N^+ for Ph_4P^+ with the intention of decreasing the spacing between the anionic chains in $[(Ph_4P)Ag(Se_4)]_n$. It was a surprise when the X-ray diffraction studies revealed that the complex crystallized with Et_4N^+ was a tetrameric discrete molecular (but homologous) compound. Furthermore, the subsequent isolation and structural characterization of yet another two different complexes with Me_4N^+ and Pr_4N^+ suggested that a variety of species of Ag^+ complexes may occur in the "primordial" DMF solution of Ag^+/Se_x^{2-} mixture which undergo complex equilibria with high lability. This is supported by the UV/vis and NMR spectroscopic data presented above.

We have noted that the variation of the nominal composition of Na_2Se_x ($x = 4$–6) used as starting material does not profoundly affect either the nature or the yield of the final products. Regardless of the polyselenide used, the complex with highest lattice stability is reproducibly isolated with a particular counterion. In other words, the type of Se_x^{2-} ligand present in the metal complex does not necessarily need to have a high equilibrium concentration in the reaction solution. The metal appears to "choose" its preferable ligand size from the equilibrium mixture of Se_x^{2-} ligands and to form a stable complex. This effect of ligand size selection by metal ions has been recognized previously in most metal/polychalcogenide systems.[1-10] We also found that the metal to ligand ratio in all these preparative reactions of the Ag^+/Se_x^{2-} series can be varied from 1:1 through 1:2 without changing the identity of the products, only the yields.

4.3. ^{77}Se NMR Studies. Solutions of I–IV, and for comparison $(Ph_4P)_2Se_5$, were investigated by ^{77}Se NMR spectroscopy at room temperature and at −55 °C in DMF. At room temperature, no well-defined signals were observed in any of the solutions, confirming the labile nature of these complexes. This suggests that even for $[Ag_4(Se_4)_3]^{2-}$, where ligand dissociation is less pronounced, considerable lability still exists probably originating from the fluxional behavior of the various rapidly exchanging modes of Se_4^{2-} ligand coordination to the Ag^+ centers and/or disproportionation. At −55 °C $[(Me_4N)Ag(Se_5)]$, $[(Ph_4P)Ag(Se_4)]_n$, and $(Ph_4P)_2Se_5$ did not show any identifiable peaks either. Interestingly, however, $[(Et_4N)Ag(Se_4)]_4$ and $(Pr_4N)_2[Ag_4(Se_4)_3]$ reveal a set of six and five broad peaks, respectively. For $[(Et_4N)Ag(Se_4)]_4$ the six peaks occur (at −55 °C) at 61, 117, 282, 590, 609, and 637 ppm, respectively. Figure 9 shows the evolution of the ^{77}Se NMR spectrum of $[(Et_4N)Ag(Se_4)]_4$ with temperature. On the basis of the structure of this complex and with the assumption that, in the pairs Se(8)/Se(4) and Se(3)/Se(7), the seleniums are in almost equivalent environments, six resonances are expected. Two of the resonances should be stronger than the other four. That is consistent with what is observed. For $(Pr_4N)_2[Ag_4(Se_4)_3]$ the five peaks occur (at −55 °C) at 5, 179, 631, 663, and 734 ppm, respectively. This pattern (see Figure 10) is hard to explain on the basis of the structure of this complex. According to the structure only four peaks would be expected. As the temperature is raised, a sixth peak appears at ~88 ppm. The spectrum disappears above 5 °C. This spectrum has been observed from different single-crystal batches. The same five-peak pattern is observed in pyridine. We do not have a satisfactory explanation for this NMR spectrum though several are possible: (a) The cluster dissociates into other unknown Ag/Se species. (b) The single crystals are really $(Pr_4N)_2[Ag_4(Se_4)_{3-x}(Se_5)_x]$ despite the fact that Se_5^{2-} fragments were not observed in the crystal structure determination. (c) The samples are in fact mixtures of $(Pr_4N)_2[Ag_4(Se_4)_3]$ and another Ag/Se phase. We believe this is unlikely because the X-ray powder diffraction patterns of the samples match well those calculated from the single-crystal structure, implying that any impurity phase is present in less than 5%. Furthermore, we prepared $(Ph_4P)_2[Ag_4(Se_4)_{3-x}(Se_5)_x]$ as reported earlier[27] and found that it also has the same ^{77}Se NMR spectrum in DMF. For comparison we also ran the ^{77}Se NMR spectra of the isostructural complex $[Cu_4(Se_4)_3]^{2-}$ from −55 to 25 °C. Surprisingly, we found that, unlike the Ag analogue, this complex is very stable, showing four narrow peaks at 218, 344, 646, and 662 ppm, respectively, as expected, at all temperatures studied (−55 to 20 °C).

4.4. Structures. This study has discovered a trend of the dependence of the Ag^+ coordination number on the size of the cations. The four Ag^+/Se_x^{2-} complexes form two structural

(38) Kräuter, G.; Weller, F.; Dehnicke, K. *Z. Naturforsch.* **1989**, *44B*, 444–454.

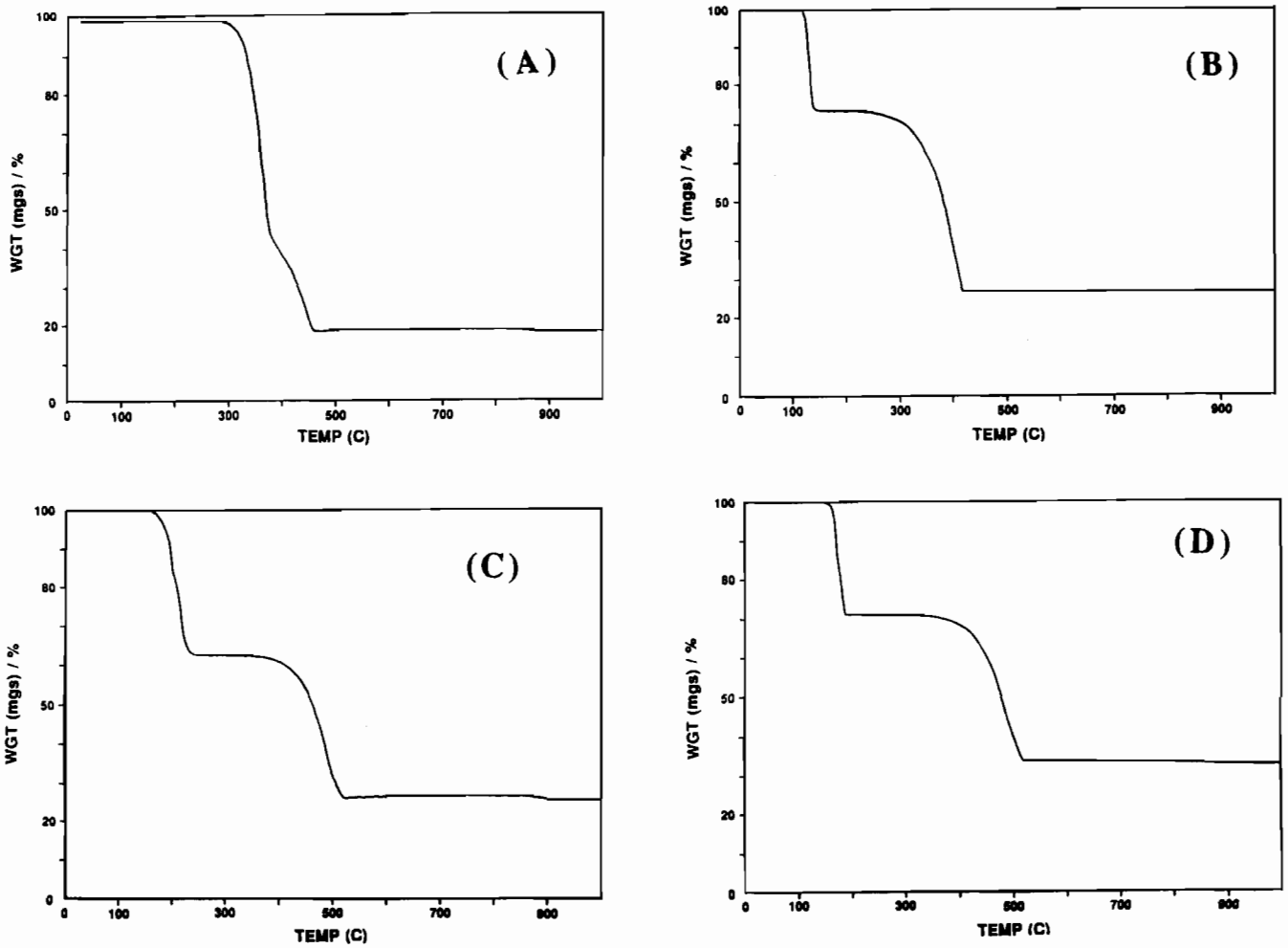

Figure 11. TGA diagrams (under nitrogen) of (A) $[(Ph_4P)Ag(Se_4)]_n$, (B) $[(Me_4N)Ag(Se_5)]_n$, (C) $[(Et_4N)Ag(Se_4)]_4$, and (D) $(Pr_4N)_2[Ag_4(Se_4)_3]$. The final product in all cases is Ag_2Se.

categories, oligomeric and polymeric. The structure of the one-dimensional compound $[(Ph_4P)Ag(Se_4)]_n$ is novel because one-dimensional inorganic polymers containing polychalcogenides are rare, particularly those obtained at ambient temperature. Among the reported one-dimensional solid-state polychalcogenides such as $(Ph_4P)_2[Hg_2Te_5]$,[13] $K_4[Ti_3S_{14}]$,[39] $Na_2[Ti_2Se_8]$,[40] NH_4CuS_4,[41] α- and β-$KCuQ_4$[42] (Q = S, Se), V_2Se_9,[43] Nb_2Se_9,[44] $Na_6Si_2Se_8$,[45] $Cs_4Sn_2Te_7$,[46] $Na_5In_2Te_6$,[47] and $[(Me_4N)Ag(S_5)]$,[26] only three, NH_4CuS_4, $(Ph_4P)_2[Hg_2Te_5]$, and $[(Me_4N)Ag(S_5)]$, are prepared at ambient temperature.

$[(Me_4N)Ag(Se_5)]_n$, $[(Et_4N)Ag(Se_4)]_4$, and $[(Ph_4P)Ag(Se_4)]_n$ can be classified as members of a whole family of compounds with the general formula $[M(Q_x)]_n^{n-}$ (M = Group 11 metal, Q = chalcogen) with homologues (but not analogues) found mostly in the polysulfide systems such as $[Ag(S_6)]_2^{2-}$,[48] $[Cu(S_6)]_3^{3-}$,[19a] $[Cu(S_4)]_3^{3-}$,[19b] and $[Cu(S_4)]_n^{n-}$.[41,42] Apparently, the two polymeric structures may be considered as end-members of the family. The tetrameric cluster $(Pr_4N)_2[Ag_4(Se_4)_3]$ does not belong to this family because of its different stoichiometry. Efforts to synthesize a family member with Pr_4N^+ were not successful.

The average Ag–Se bond distance in each Ag^+/Se_x^{2-} complex depends on the Ag^+ coordination geometry, as expected. The longest average Ag–Se bond of 2.677 (27) Å is found in $[(Me_4N)Ag(Se_5)]_n$, where the Ag^+ ions adopt a coordination number of 4. The shortest average Ag–Se bond of 2.590 (41) Å is observed in $[(Ph_4P)Ag(Se_4)]_n$, in which the coordination number for the Ag atoms is 3. Complexes III and IV exhibit intermediate Ag–Se bonds of 2.669 (42) and 2.604 (15) Å, respectively. This systematic variation of Ag–Se bond distances correlates well with the Ag^+ coordination number as expected. In spite of different molecular structures, all the four Ag^+ polyselenide complexes can be derived by using the five-membered $AgSe_4$ rings as basic building blocks. The conformation of the MQ_4 five-membered rings might be described as either "envelope" or "half-chair", with analogy to the conformations of cyclopentane. The majority of the $AgSe_4$ rings in these polyselenides adopt the envelope conformation, which is relatively common in the metal polychalcogenide systems containing MQ_4 rings.

The $[Ag(Se_4)]_n^{n-}$ chain bears a structural relationship to the α-$[Cu(S_4)]_n^{n-}$[42] chain. For instance, both polymers are composed of MQ_4 five-membered rings, which generate each other by a crystallographic 2-fold screw axis parallel to the chain direction. This leads to the zigzag array of metal atoms along the chain. Yet, the coordination geometries of the metal ions in these two structures exhibit a significant difference. In $[Ag(Se_4)]_n^{n-}$, Ag^+ is trigonal planar, while, in α-$[Cu(S_4)]_n^{n-}$, Cu^+ is tetrahedral. This difference is caused by the different size of counterion in each structure. One can view $[Ag(Se_4)]_n^{n-}$ as being formed by "stretching" a hypothetical α-$[Ag(Se_4)]_n^{n-}$ chain isostructural to

(39) Sunshine, S. A.; Kang, D.; Ibers, J. A. *J. Am. Chem. Soc.* **1987**, *109*, 6202–6204.
(40) Kang, D.; Ibers, J. A. *Inorg. Chem.* **1988**, *27*, 549–551.
(41) Burschka, C. *Z. Naturforsch.* **1980**, *B35*, 1511–1513.
(42) Kanatzidis, M. G.; Park, Y. *J. Am. Chem. Soc.* **1989**, *111*, 3767–3769.
(43) Furuseth, S.; Klewe, B. *Acta Chem. Scand.* **1984**, *A38*, 467–471.
(44) Meerschaut, A.; Guemas, L.; Berger, R.; Rouxel, J. *Acta Crystallogr., Sect. B* **1979**, *B35*, 1747–1750.
(45) Eisenmann, B.; Hansa, J.; Schäfer, H. *Z. Anorg. Allg. Chem.* **1985**, *526*, 55–59.
(46) Brinkmann, C.; Eisenmann, B.; Schäfer, H. *Mater. Res. Bull.* **1985**, *20*, 299–305.
(47) Eisenmann, B.; Hofmann, A.; Zagler, R. *Z. Naturforsch.* **1990**, *45B*, 8–14.
(48) Müller, A.; Römer, M.; Bögge, H.; Krickemeyer, E.; Baumann, F.-W.; Schmitz, K. *Inorg. Chim. Acta* **1984**, *89*, L7–L8.

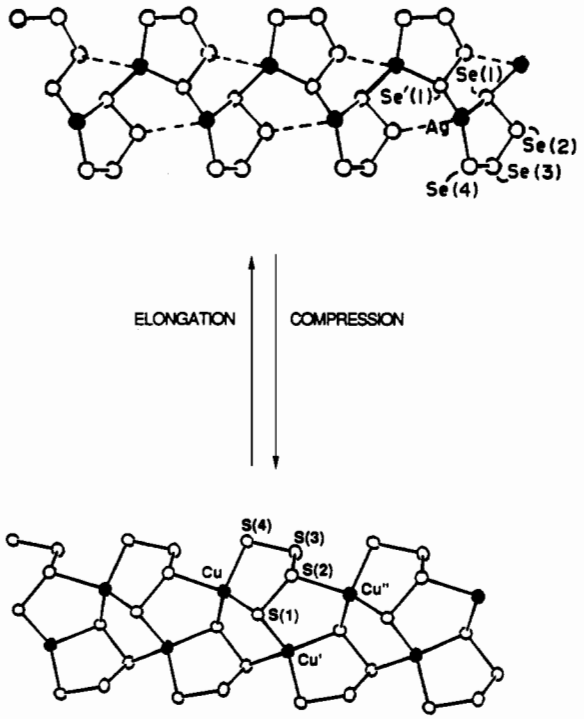

Figure 12. Structural relationship of α-$[Cu(S_4)]_n^{n-}$ and $[Ag(Se_4)]_n^{n-}$. The dotted lines in $[Ag(Se_4)]_n^{n-}$ indicate the Ag–Se distances to be shortened upon compression of this structure along the chain axis. The Ag atom will attain a tetrahedral coordination geometry.

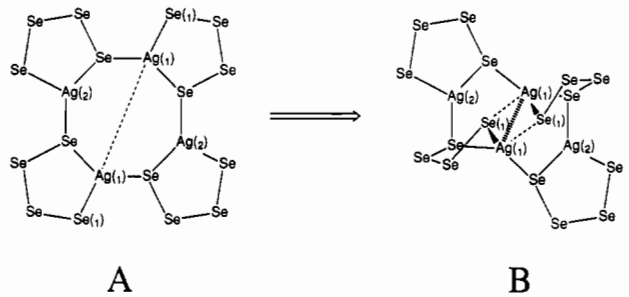

Figure 13. Formation of the $[Ag(Se_4)]_4^{4-}$ cluster B from the hypothetical c-$[Ag(Se_4)]_4^{4-}$ cluster A upon switching on d^{10}–d^{10} contacts between the diametrically disposed Ag(1) atoms. Since there are more bonds in cluster B, its volume will be smaller than that of cluster A.

α-$[Cu(S_4)]_n^{n-}$ along the chain direction. Conversely, "compressing" $[Ag(Se_4)]_n^{n-}$ along the chain direction will expand the Ag coordination sphere from three to four by bringing the Se(2) atom close to Ag. This is shown in Figure 12. The stretching effect may result from the replacement of K^+ for Ph_4P^+, as the substitution of large cation for small one must cause the expansion of the structure in each direction, including the chain direction which breaks the "bond" between Se(2) and Ag'. Unfortunately, attempts to prepare α-NH_4AgSe_4 or α-$[KAg(Se_4)]_n$ thus far have been unsuccessful. The closest we could come to a small cation was Me_4N^+. The one-dimensional $[(Me_4N)Ag(Se_5)]_n$ indeed has a tetrahedral Ag^+ center even though the Se_x^{2-} ligand is different.

The structure of $[(Et_4N)Ag(Se_4)]_4$ is new, and it has no polysulfide analogue. It is interesting that III does not adopt the structure schematically shown in Figure 13, which would be homologous to the cyclic $[Cu(S_6)]_3^{3-}$.[19a] Nevertheless, the actual structure of III can be derived from that shown in Figure 11 by "turning on" a d^{10}–d^{10} attractive interaction between two diametrically opposite Ag^+ atoms. This will bring the two silver atoms close, deforming the square array of Ag atoms into a rhombus. Further bridging (ternary interaction) from coordinated Se(1) atoms would expand the silver coordination sphere from three to four. The ternary bridging Se(1)–Ag(1) interactions may be a consequence of the counterion size, which causes the complex to assume a certain volume appropriate for crystal packing. The individual ternary Se(1)–Ag(1) interactions which result in the long Se–Ag bonds may be modulated by fine tuning in the counterion volume (e.g. use of slightly different cations such as Et_3NPr^+ and $Et_2NPr_2^+$). Isolation of Ag/Se complexes with such cations is now in progress.

In $(Pr_4N)_2[Ag_4(Se_4)_3]$, four Ag atoms are "glued" together by three Se_4^{2-} ligands of total twelve coordination bonds toward Ag atoms with each Ag atom assuming trigonal-planar coordination geometry (CN = 3). The bridging nature of Se_4^{2-} ligands in $(Pr_4N)_2[Ag_4(Se_4)_3]$ and $[(Et_4N)Ag(Se_4)]_n$ is essentially the same as that commonly found in group 11 metal polysulfide clusters (i.e. Ag and Cu).

By comparison of the coordination geometries of Ag atoms in these four complexes, it is clear that the coordination sphere of Ag^+ ion in each compound depends to a large extent upon the size of the counterion. For large cations such as Ph_4P^+ and Pr_4N^+, the Ag atoms assume the lower coordination number of 3, while a small cation such as Me_4N^+ favors the higher coordination number of 4 for the Ag atoms. Interestingly, an intermediate size cation such as Et_4N^+ results in two types of coordination geometries of Ag atoms distorted tetrahedral and trigonal planar in II. The average coordination number in II can be regarded as intermediate of 3.5. An example of a metal/chalcogen system that shows a similar counterion dependence is the ethylenediamine-extracted solution of an alloy with the composition of $K_2Hg_2Te_3$,[13] from which two complexes were crystallized through the use of two different organic cations. The one-dimensional polymeric anion $[Hg_2Te_5]_n^{2n-}$ can be isolated by using the large cation Ph_4P^+. The polymeric chains of the anions feature a trigonal-planar Hg atom, while the tetrahedrally coordinated Hg atoms are found in the tetrameric cluster of $[Hg_4Te_{12}]^{4-}$, which was crystallized with the somewhat smaller cation n-Bu_4N^+. It should be noted however that a counterion effect on the final crystallization products of M^{n+}/polychalcogenides, where $n \geq 2$, is not very pronounced and other parameters become important such as the M^{n+}/Q_x^{2-} ratio.[49] The influence of counterion on the structure of the anion has been known for some Mo/S_x^{2-} systems.[7b] However, no particular trend has been identified. A systematic dependence of the metal coordination number upon the size of counterion has been noticed in some group 11/halide systems.[50]

The Ag^+ coordination number/size of counterion correlation in the series of compounds reported here prompted us to review the literature for similar effects in other known group 11 metal/polychalcogenide complexes. Indeed, the Cu^+, Ag^+, and Au^+/S_x^{2-} systems also follow this correlation. For example, the Cu^+ coordination number (CN) found either in NH_4CuS_4 or α- and β-$KCuS_4$ is 4. The cations NH_4^+ and K^+ can be considered as very small compared to the organic quaternary ammonium or phosphonium cations. The Cu^+ coordination number in $(Ph_4P)_2(NH_4)[Cu_3(S_4)_3]$[19] and $(Ph_4P)_4[Cu_2S_{20}]$[51] is 3, as both compounds contain the large cation Ph_4P^+. Several known silver(I) polysulfide compounds have been isolated with various organic cations such as Me_4N^+, $(Ph_3PNPPh_3)^+$, Ph_4As^+, and Ph_4P^+. These are $[(Me_4N)Ag(S_5)]_n$ (CN = 4),[26] $(Ph_4P)_4[Ag_2S_{20}]$ (CN = 3),[52] $(Ph_4P)_2[Ag_2(S_6)_2]$ (CN = 3),[53] $(Ph_3PNPPh_3)[Ag(S_9)]\cdot S_8$

(49) Kim, K.-W.; Dhingra, S.; Kanatzidis, M. G. Manuscript in preparation.
(50) (a) Andersson, S.; Jagner, S. *Acta Chem. Scand., Ser. A* **1988**, *A42*, 691–697. (b) Andersson, S.; Jagner, S. *Acta Chem. Scand., Ser. A* **1987**, *A41*, 230–236. (c) Andersson, S.; Jagner, S. *Acta Chem. Scand., Ser. A* **1986**, *A40*, 52–57. (d) Jagner, S.; Olson, S.; Stomberg, R. *Acta Chem. Scand., Ser. A* **1986**, *A40*, 230–232. (e) Andersson, S.; Jagner, S. *Acta Chem. Scand., Ser. A* **1986**, *A40*, 210–217. (f) Andersson, S.; Jagner, S. *Acta Chem. Scand., Ser. A* **1985**, *A39*, 423–428. (g) Andersson, S.; Jagner, S. *Acta Chem. Scand., Ser. A* **1985**, *A39*, 799–812. (h) Andersson, S.; Jagner, S. *Acta Chem. Scand., Ser. A* **1985**, *A39*, 515–520. (i) Asplund, M.; Jagner, S.; Nilsson, M. *Acta Chem. Scand., Ser. A* **1985**, *A39*, 447–451. (j) Andersson, S.; Jagner, S. *Acta Chem. Scand., Ser. A* **1985**, *A39*, 181–186. (k) Asplund, M.; Jagner, S. *Acta Chem. Scand., Ser. A* **1985**, *A39*, 47–51. (l) Andersson, S.; Jagner, S. *Acta Chem. Scand., Ser. A* **1985**, *A39*, 177–181.
(51) Müller, A.; Baumann, F.-W.; Bögge, H.; Römer, M.; Krickemeyer, E.; Schmitz, K. *Angew. Chem., Int. Ed. Engl.* **1984**, *23*, 632–633.

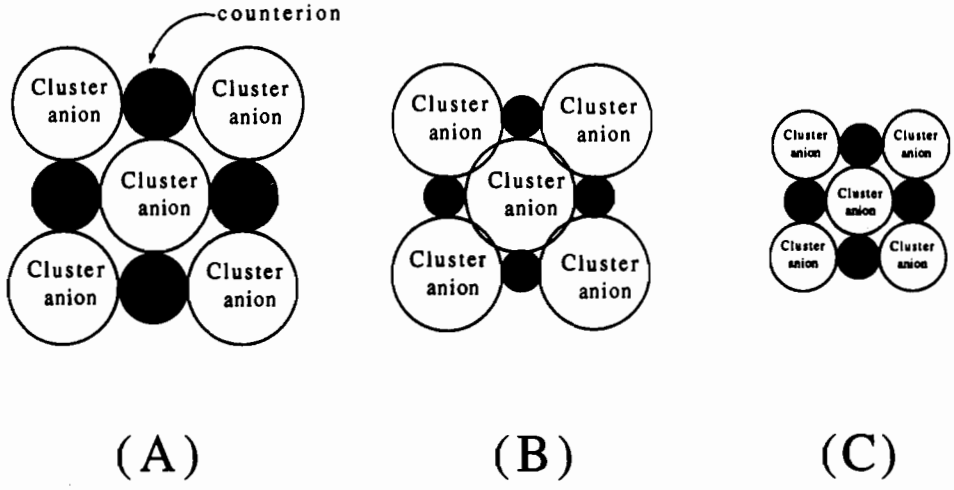

Figure 14. Schematic depiction of how the anion volume can adjust to accommodate changes in the cation volume in order to maintain a stable lattice: (A) hypothetical cation–anion stable crystalline assembly; (B) assembly showing that substitution of the cation in (A) with a smaller cation will bring the anions too close together, thus experiencing destabilizing anion–anion repulsions; (C) assembly showing that if the anion can decrease its volume (e.g. by increasing intraatomic bonding), a stable lattice can be attained again with the smaller cation.

(CN = 2).[54] For Au^+, there are two complexes, $(Ph_4P)_2[Au_2S_8]$ (CN = 2)[53] and $(Ph_4As)[Au(S_9)]$ (CN = 2).[19d] Notice that the largest cation, $Ph_3PNPPh_3^+$, favors the smallest CN. Unfortunately, no structurally characterized gold(I) polysulfides containing smaller cations are available at this time to examine this dependence further.[55]

Although a clear explanation of this effect is not available, we wish to note the following. The size of the $[Ag_xSe_y]^{n-}$ anions will have to follow the size of the counterion in order to form a stable crystal lattice. It is not unreasonable to consider that amidst a collection of various possible $[Ag_xSe_y]^{n-}$ anion clusters a small cation may need a smaller cluster to form a stable lattice. Within a given nuclearity $[Ag_xSe_y]^{n-}$ cluster, different molecular volumes may be attainable by just adjusting the silver CN. High CN will produce compact structures, while small CN will result in expanded structures. In order to crystallize these polychalcogenide anions, the cations must find an efficient way to screen the anions from one another in the lattice. Failure to do so will result in an unstable lattice due to anion–anion repulsive interactions. This is schematically shown in Figure 14. If the volume of the cation becomes significantly smaller (see Figure 14) to the point where the anions are no longer screened effectively, repulsive Coulombic forces will become operative. If another satisfactory lattice cannot be found, then an alternative for the anions would be to decrease their molecular volume accordingly so that screening by the smaller cations can resume. The best way to decrease the anion volume while keeping the stoichiometry or composition constant is to increase the number of intracluster bonds and thus to expand the metal coordination sphere. This would be particularly likely with labile clusters such as those of group 11 metals. Figure 13 also illustrates the aforementioned point where the hypothetical anion on the left has a larger molecular volume than that of the right. We expect the metal coordination sphere/counterion size correlation will also apply to related systems such as Cu^+/Se_x^{2-} and Au^+/Se_x^{2-}.[56]

5. Concluding Remarks

The reaction of pentaselenide anion, Se_5^{2-}, with silver nitrate in the presence of various large organic cations (i.e. Me_4N^+, Et_4N^+, Pr_4N^+, and Ph_4P^+) in DMF provides a convenient access to several new silver(I) polyselenide complexes: $[(Ph_4P)Ag(Se_4)]_n$, $[(Me_4N)Ag(Se_5)]_n$, $[(Et_4N)Ag(Se_4)]_4$, and $(Pr_4N)_2[Ag_4(Se_4)_3]$. The structures of this series of silver(I) polyselenide complexes show a great deal of diversity, ranging from one-dimensional solid-state polymers to discrete tetrameric molecules. The nature of the anionic complexes entirely depends on the characteristics of their counterions. A systematic variation of Ag coordination sphere with the size of the counterions has been recognized in this Ag^+/Se_x^{2-} system and other previously reported group 11/polysulfide systems. The smaller the counterion, the greater the metal coordination number. The isolation of four different compounds from the same DMF solution of a Ag^+/Se_x^{2-} mixture attests to the facile and complex equilibria between different Ag^+/Se_x^{2-} species. Given the fact that the Ag^+/Se_x^{2-} system has fairly complicated solution chemistry and that all the spectroscopic techniques available do not provide structural information, the structural characterization by X-ray single-crystal analysis is indispensable for the investigation of silver(I) polyselenide and related chemistry.

Acknowledgment. Financial support from the Center for Fundamental Materials Research (CFMR) at Michigan State University and the donors of the Petroleum Research Fund, administered by the American Chemical Society, is gratefully acknowledged. The NMR data were obtained on instrumentation purchased in part with funds from NIH Grant 1-S10-RR04750-01 and from NSF Grant CHE-88-00770.

Supplementary Material Available: Tables of atomic coordinates of all atoms, anisotropic and isotropic thermal parameters of all non-hydrogen atoms, and crystallographic and structure refinement data for $[(Ph_4P)Ag(Se_4)]_n$, $[(Me_4N)Ag(Se_5)]_n$, $[(Et_4N)Ag(Se_4)]_4$, and $(Pr_4N)_2[Ag_4(Se_4)_3]$ (26 pages); listings of calculated and observed $10F_o/10F_c$) structure factors for $[(Ph_4P)Ag(Se_4)]_n$, $[(Me_4N)Ag(Se_5)]_n$, $[(Et_4N)Ag(Se_4)]_4$, and $(Pr_4N)_2[Ag_4(Se_4)_3]$ (81 pages). Ordering information is given on any current masthead page.

(52) Müller, A.; Krickemeyer, E.; Zimmermann, M.; Römer, M.; Bögge, H.; Penk, M.; Schmitz, K. *Inorg. Chim. Acta* **1984**, *90*, L69–L71.
(53) Müller, A.; Römer, M.; Bögge, H.; Krickemeyer, E.; Zimmermann, M. *Z. Anorg. Allg. Chem.* **1986**, *534*, 69–76.
(54) Marbach, G.; Strähle, J. *Angew. Chem., Int. Ed. Engl.* **1984**, *23*, 246–247.
(55) (a) Recently, two new nonsoluble Au^+ polychalcogenides, $KAuQ_5$ (Q = S, Se), obtained by a molten salt method seem to violate the above correlation. The two polymeric compounds are isostructural to each other, formed by bridging linearly coordinated Au^+ ions with Q_5^{2-} chains. In spite of the small cation K^+ occurring in the structures, the Au^+ does not adopt the higher coordination number as expected. The compounds, however, contain significant interchain Au···Au interactions, which, in combination with the well-known strong preference of Au^+ for linear coordination, account for this deviation. (b) Park, Y.; Kanatzidis, M. G. *Angew. Chem., Int. Ed. Engl.* **1990**, *29*, 914–915.
(56) (a) The reaction of the Se_x^{2-} anions with CuCl in DMF in the presence of Ph_4P^+ resulted in the isolation of a pure crystalline product. The X-ray structural analysis revealed trigonal-planar Cu^+ atoms and the composition $(Ph_4P)_4[(Se_x)Cu(Se_6)Cu(Se_y)]$ (x, y = 4, 5). The syntheses of copper(I) polyselenide complexes with small- and intermediate-size organic cations are currently under way. (b) Huang, S.-P.; Dhingra, S.; Kanatzidis, M. G. Unpublished results. (c) Müller, U.; Ha-Eierdanz, M.-L.; Kräuter, G.; Dehnicke, K. *Z. Naturforsch.* **1990**, *45b*, 38–42.